

**A**  
**Project Report**  
**On**  
**Studies on Hydrodynamic Behaviour and COD Removal**  
**Efficiency using Inverse Fluidised Bed Bioreactor: Statistical**  
**Analysis**

A Report Submitted in Partial Fulfillment for the Requirements of the Degree of  
**Master of Technology**  
**In**  
**Chemical Engineering**

Submitted By  
**Tanmaya Lima**  
**Roll no. - 210CH1202**

Under the Guidance of  
**Prof. Abanti Sahoo**



**Department of Chemical Engineering**  
**National Institute of Technology,**  
**Rourkela-769008, India**



## CERTIFICATE

This is to certify that the project report entitled, “**Studies on Hydrodynamic Behaviour And COD Removal Efficiency using Inverse Fluidised Bed Bioreactor: Statistical Analysis** ” submitted by **Tanmaya Kumar Lima** (210CH1202) in partial fulfilment of the requirements for the award of Master of Technology Degree in Chemical Engineering at the National Institute of Technology, Rourkela is an authentic work carried out by him under my supervision and guidance.

To the best of my knowledge, the matter embodied in the report has not been submitted to any other University/Institute for the award of any Degree.

Date:

---

Signature of the Supervisor

**Name: Prof. Abanti Sahoo**

**Designation:** Associate Professor

**Department:** Chemical Engineering

National Institute of Technology, Rourkela

Rourkela-769008, Odisha

## ACKNOWLEDGEMENT

I feel immense pleasure and privilege to express my deep sense of gratitude and feel indebted towards all those people who have helped, inspired and encouraged me during the preparation of this report.

I am grateful to my supervisor, **Prof. Abanti Sahoo**, for her kind support, guidance and encouragement throughout the project work, also for introducing to this topic. I would also like to thank HOD, **Prof. R. K. Singh** for his kind help to make this report complete. I am also thankful to all the staff and faculty members of Chemical Engineering Department, National Institute of Technology, Rourkela for their consistent encouragement. I would also like to extend my sincere thanks to my senior especially to Mr. Suman Choudhury & Mr. Rajesh Tripathy for his unconditional assistance and support.

Last but not the least, I would like to thank whole heartedly my parents and family members whose love and unconditional support, both on academic and personal front, enabled me to see the light of this day.

Thanking You,

**TANMAYA LIMA**

Roll No.210CH1202

# ***CONTENTS***

<b>Serial no.</b>	<b>Items</b>	<b>Page No</b>
	List of Tables	v
	List of Figures	vi
	Abstract	1
<b>1</b>	<b>Chapter 1 - INTRODUCTION</b>	<b>2-5</b>
1.1	Inverse Fluidisation	3
1.2	Advantages of Inverse Fluidisation process	3
1.3	Application of IF in waste water Treatment:	4
1.4	Objective of the work	4
1.5	Thesis Layout	5
<b>2</b>	<b>Chapter 2 - LITERATURE SURVEY</b>	<b>6 - 20</b>
2.1	Studies on hydrodynamic behaviour of inverse fluidised bed	8
2.1.1	Bed expansion	8
2.1.2	Gas holdup	10
2.1.3	Solid holdup	11
2.1.4	Liquid holdup	11
2.1.5	Minimum fluidization velocity	12
2.2	Chemical oxygen demand	12
2.3	Biochemical oxygen demand	13
2.4	Previous work on IFBB	14
2.5	Factorial design	18
<b>3</b>	<b>CHAPTER 3 - EXPERIMENTATION</b>	<b>21 - 32</b>
3.1	Experimental setup	22
3.2	Specifications of Equipment Parts	24
3.3	Experimental procedure	24
3.4	Biological Treatment Of Waste Water	25
<b>4</b>	<b>Chapter 4 – RESULTS AND DISCUSSIONS</b>	<b>32 - 54</b>

4.1	Hydrodynamic studies	33
4.2	Studies on COD removal efficiency	45
5	<b>Chapter 5 - CONCLUSION</b>	55-56
	<b>NOMENCLATURES</b>	58
	<b>REFERENCES</b>	69

---

## LIST OF TABLES

<b>Table No.</b>	<b>Items</b>	<b>Page No.</b>
Table 3.1	Physical properties of some particles	29
Table 3.2	Scope of experiment for hydrodynamic studies	30
Table 3.3	Scope of experiment for COD removal efficiency	31
Table 4.1	Holdups at different static bed heights	53
Table 4.2	Properties of sample-2 (steelplant effluents) after treatment.	53
Table 4.3	Initial and final TOC of pondwater	53
Table 4.4	Observed data & comparison of calculated values of pressure drop with experimental values.	54
Table 4.5	Observed data & comparison of calculated values of % COD removal efficiency with experimental values	55
Table 4.6	Standard deviation and Mean deviation of calculated values with experimental values.	56

## LIST OF FIGURES

<b>Fig. No.</b>	<b>Items</b>	<b>Page No.</b>
Fig.1	Set up of inverse fluidised bed	23
Fig 2.	Bed height versus liquid velocity for different bed weight.	34
Fig 3	Liquid velocity versus void fraction.	35
Fig 4	Pressure drop profile for static bed height of 12cm (100 gm of bed weight)	35
Fig 5	Pressure drop versus liquid velocity for bed weight 100 gms.	36
Fig.6	pressure variation versus bed height	36
Fig.7	Pressure drop profile at various air flow rate	37
Fig.8	Comparison of pressure drop for different distributor for manometer 1	37
Fig.9	Comparison of pressure drop through manometer 1 for different static bed height	38
Fig.10	Pressure drop vs. liquid velocity	38
Fig.11	Correlation plot of pressure drop against system parameter	39
Fig.12	Overall column pressure drop against water flow rate	40
Fig.13	Overall column pressure drop against air flow rate	40
Fig.14	Pressure drop at different levels in the column	41
Fig.15	Gas holdup profile against static bed heights	41
Fig.16	Gas holdup vs. gas flow rate	42
Fig.17	Gas holdup vs. water flow rate	42
Fig.18	Liquid holdup vs. static bed heights	42

Fig.19	Bed height vs. solid holdup	43
Fig. 20	Holdup profiles against static bed height	44
Fig.21	Comparison of pressure drop between pond and tap water	44
Fig. 22	Optical density at regular intervals at 580nm of visible light	46
Fig. 23	Growth kinetics of <i>pseudomonas aeruginosa</i> culture	47
Fig.24	Dependence of COD values on time (t) for ratio ( $V_b/V_R$ ) = 0.50 and various oxygen velocities (u).	48
Fig. 25	Relationship between COD values and time (t) for ratio ( $V_b/V_R$ ) = 0.55 and various oxygen velocities (u).	49
Fig.26	Dependence of COD values on time (t) for ratio ( $V_b/V_R$ )= 0.60 and various oxygen velocities (u).	49
Fig.27	Comparison of cod removal at optimum condition	50
Fig.28	COD removal efficiency for continuous culture mode at optimum conditions.	51
Fig.29	Comparison of COD removal efficiency of batch culture mode with continuous mode.	51
Fig.30	Correlation plot of percentage COD removal against system parameter	52

---



## **ABSTRACT**

Current worldwide commercial activities for the treatment of industrial effluents and the waste water prompt the researchers to use inverse fluidization technique for the simplicity of the process, easy handling, low process cost, low energy consumption and high efficiency as compared to normal fluidization technique. Therefore further fundamental research in hydrodynamic behaviour, effects of different parameters, correlation development and the scale up effects of three-phase inverse fluidization systems have been planned to be studied in this work. The present work summarizes the salient characteristics of hydrodynamics behaviour of inverse fluidized system, effect of particles properties, fluid velocity and its various uses in commercial scale. Hydrodynamic behaviour of the IFB (inverse fluidized bed) in terms of the bed pressure drop by varying different system parameters (viz. air flow rate, water flow rate, and static bed height and orifice diameter on the distributor plate) has been studied experimentally. Pressure drop profiles, voidage profiles and the fluidization velocity profiles for the IFB have been studied. COD and BOD analysis has also been carried out for the RSP waste water. The system parameters such as oxygen flow rate, bed volume, residence time are optimised for maximum COD reduction.

# **CHAPTER-1**

## **INTRODUCTION**

## **1.1 Inverse Fluidisation**

When the density of the particles is smaller than that of the liquid, fluidization can be achieved with downward flow of the liquid counter to the net upward buoyancy force on the particles. In this type of process the gas flow is upward, counter to the liquid flow. This type of fluidization is termed inverse fluidization. Inverse Fluidized Beds can be operated as two- (liquid-solid) or three- (gas-liquid-solid) phase systems.

Liquid fluidization technologies have received large attention because of the development of newer application fields, mainly biochemical processing and waste-water treatment. Liquidó solid fluidization generally operates with an upward flow of liquid using particles of higher density than the liquid. Inverse fluidization is a phenomenon where the particles, which have a density lower than that of the liquid, are fluidized by a down-flow of the liquid. The inverse fluidization system has gained significant importance during the last decade in the field of environmental, biochemical engineering, and oilówater separation. The advantages compare to normal fluidization inverse fluidization in biochemical engineering are that it can control biofilm thickness in a very narrow range. As the solids can be fluidized at low liquid velocity, the energy expenditure is low and also the solids attrition is minimum. The other advantages are the high mass transfer rates, minimum carryover of coated microorganisms due to less solids attrition than normal fluidization and ease of re-fluidization in case of power failure.

## **1.2 Advantages of Inverse Fluidisation process**

Current worldwide commercial activities for the treatment of industrial effluents and the waste water from many industries like wine industry, distillery industry, sugar industry use inverse fluidization technique for their simplicity in process, easy to handle , low cost process ,low energy consumption and efficient as compare to normal fluidization technique. Such commercial activities have prompted further fundamental research interest in hydrodynamic behaviour, effects of different parameters, various correlations and the scale up effects of three-phase inverse fluidization systems. The advantages of this new contacting pattern are large gas holdups, low fluid velocity, small energy, easy fluidization without breakage of solid particles, high rates of heat and mass transfer, low attrition of solid particles, and easy re-fluidization in

case of power failure. The gas flow is upward, counter to the liquid flow and bed expansion can be supported either by the downward liquid phase or by the upward gas phase, or by both in a three phase fluidized bed.

### **1.3 Application of IF in waste water Treatment:**

The application of inverse fluidization technique in biotechnology is one of the most important areas in bioreactor engineering. The waste water (WW) treatment is a process of removing contaminants and organic material from WW using various techniques, systems and methods. Several physical, chemical and biological methods have been used for the treatment of WW. The quality of a good WW treatment system is indicated or determined by the higher pollutant degradation/mineralization efficiency with cost effectiveness and ease of operation. The various advantages of IF lead to its application in WW treatment. IF has been a powerful tool in the treatment of waste water from various wine, distillery and sugar industries.

The uncontrolled growth of the fixed biomass changes the hydrodynamics of the particles as well as the whole-fluidized bed. To avoid this and the fast consumption of oxygen in a two-phase fluidized bed, the concept of inverse fluidization is used. Inverse fluidization plays a vital role in achievement of the bio-film thickness control in a very narrow range.

The main interest of hydrodynamics modeling approach in a context of fluidized bed bioreactor modeling is to calculate the fluidization characteristics such as holdup and velocity of each phase present in the reactor, due to their influence on the system residence time, reactor size, specific bio-film superficial area, mass transfer and bio-film detachment processes. Indeed, characteristics of fluidization in a bioreactor are functions of bio-film concentration.

### **1.4 Objective of the work**

The aim of this work is to evaluate the feasibility of an inverse fluidized bed reactor for the aerobic digestion of industrial effluent, with a carrier material that allows low energy requirements for fluidization thereby providing a large surface for biomass attachment and development. COD (chemical oxygen demand) reduction in the industrial effluents is also aimed for various ratios of settled bed volume to reactor volume, air velocities, water flow rate and mean residence times.

The aim of the present work could be summarized as follows:

- ❖ To study the effect of different system parameters on hydrodynamic behaviours of the inverse fluidized bed thereby correlating the different system parameters with the experimentally observed data.
- ❖ Study the feasibility of an inverse fluidized bed reactor for the aerobic digestion of industrial effluent.
- ❖ Finding optimum parameters of bioreactor operation for maximum COD removal.

### **1.5 Thesis Layout**

The project work has been reported in six chapters. Chapter-1 deals with the introduction regarding behaviour of the inverse fluidised bed and its application for waste water treatment. Chapter-2 deals with the literature surveys on previous works with respect to the hydrodynamic behavior of the inverse fluidized bed bioreactor in which the working principles, effects of various parameters, its applications as a bioreactor and other research works are discussed. The third chapter deals with the experimental aspects of inverse fluidized bed. Schematic diagram and methodology of the experiments. Chapter-4 described results and discussion. Experimental observations are also presented here. The results of the experiment are summarized based on which discussion has been carried out for the optimisation of different parameters used in the experiment. The final chapter gives the summary of the conclusion.

## **CHAPTER-2**

## **LITERATURE REVIEW**

A bioreactor may refer to any manufactured or engineered device or system that supports a biologically active environment. A bioreactor is a vessel in which a chemical process is carried out which involves organisms or biochemically active substances derived from such organisms. This process can either be aerobic or anaerobic.

Bioreactors can also be used to treat sewage and wastewater. In the most efficient of these systems there is a supply of free-flowing, chemically inert media that acts as a receptacle for the bacteria that breaks down the raw sewage. Examples of these bioreactors often have separate, sequential tanks and a mechanical separator or cyclone to speed the division of water and bio-solids. Aerators supply oxygen to the sewage and media further accelerating breakdown. Submersible mixers provide agitation in anoxic bioreactors to keep the solids in suspension and thereby ensure that the bacteria and the organic materials come in contact with each other. In the process, the liquids organic pollutant measuring parameters like Biochemical Oxygen Demand (BOD) & COD (chemical oxygen demand) is reduced sufficiently to render the contaminated water fit for reuse. Because the microorganisms are the engine that drives biological wastewater treatment, it is critical to closely monitor the quantity and quality of microorganisms in bioreactors.

Fluidised bed bioreactors present a number of advantages that renders them suitable as an attractive alternative to treat waste water. Three phase inverse fluidised beds have gained a considerable application in chemical, wastewater treatment and in biochemical industries. Some of the reasons for their extensive use are simplicity in construction, low maintenance due to lack of moving parts, high effective interfacial areas and therefore, a high heat and mass transfer per unit volume. Particularly, there is an increasing use of inverse phase fluidised bed bioreactors and bubble columns in biological treatment of wastewater. This is as a result of a need for a more specialised method of treatment for industrial wastewaters, which occasionally contain volatile toxic components. Treatment of these toxic substances in open lagoons could be a health hazard; therefore, the fluidised bed bioreactor becomes a system of choice. The geometry of the reactor is dictated by the characteristics of the waste to be treated.

One of the principal requirements for a bioreactor is the ability of the micro-organisms to grow on the support particle and remain embedded for significant biodegradation to take place.

The microbial growth rate is so crucial for bioreactor performance that a lot of attention has been given to this, owing to the fact that bed turbulence and the nature of support particle appreciably affect microbial attachment. Considering the nature of the waste, it has been found necessary to adjust nutrient content and pH to enable initial microbial growth. Gas and oxygen flow rate affects phase mixing and gas hold ups, which are important parameters that influence oxygen mass transfer. The survival as well as the activity of the aerobic micro-organisms depends on the amount of oxygen dissolved. A well mixed medium will give rise to a homogeneous bed that promotes interfacial mass transfer and this will make oxygen available to the micro-organisms.

Inverse gas-liquid-solid beds are most effective when the density of the particles and the liquid are close since they are easily fluidized with a smaller liquid recycle ratio. The expanded bed height obtained from the conductivity method increased as either the liquid or the gas velocity is increased. From the available literature it is observed that only limited studies are reported in two-phase inverse fluidized bed reactor with reference to bed expansion and pressure drop studies.

## 2.1 Studies on hydrodynamic behaviour of inverse fluidised bed

It is essential to know about the bed dynamics for a better design of the bioreactor by which reactor efficiency is improved in a cost-effective manner. Hydrodynamic studies give informations on bed dynamics such as bed pressure drop, bed expansion, phase hold ups and minimum fluidization velocity of the selected system.

**2.1.1 Bed expansion:** Three types of model has been suggested by **Fan et al. (1982)**, First type correlations for the bed expansion are expressed in a relationship between  $U_a$  and  $\epsilon$ , which is theoretical, semi-theoretical or empirical in nature.

Second type correlations for the bed expansion have been developed by modifying the relation between the drag coefficient and Reynolds number for a single particle.

Third type of correlation for bed height has been directly correlated with operating liquid velocity, particle diameter and density.

Based on the first type model, the following empirical relations have been obtained by the authors for the bed voidage in the inverse fluidized system:

$$U_R = \epsilon^n \quad (1)$$



Where,  $n = 15 \text{Re}_t^{-0.35} \exp(3.9d/D)$ ; for  $350 < \text{Re}_t < 1250$

$$n = 0.86 \text{Re}_t^{-0.2} \exp(-0.75d/D) ; \quad \text{for } \text{Re}_t > 1250$$

Based on the second type model the drag force function (f) for the multiparticle system can be expressed in terms of the Archimedes number 'Ar' as:

$$f = Ar / 13.9 \text{Re}^{1.4}, (2 < \text{Re} < 500) \quad (2)$$

$$f = 3Ar / \text{Re}^2, (\text{Re} > 500) \quad (3)$$

$$\text{Where } Ar = d^3(\rho_l - \rho_s)\rho_l g / \mu_l^2$$

An empirical correlation for the function 'f' in terms of  $\varepsilon$ , Ar and d/D developed by **Fan et al. (1982)** for inverse liquid-solid fluidization is expressed as follows:

$$f = 3.21\varepsilon^{-4.05} Ar^{-0.07} \exp 3.5d/D \quad (4)$$

The coefficient of variation for eq(4) has been observed to be within 15%. Thus the range of applicability of eqn.(4) :  $\varepsilon = 0.40$  to  $0.88$ ,  $Ar = 1.1 \times 10^5$  to  $7.65 \times 10^6$ ,  $d/D = 0.062$  to  $0.250$ .

The bed expansion in the down comer has been investigated by Han et al. (2000). There are different models for the correlation of bed expansion with the superficial liquid velocity. Among all these correlations, the model proposed by **Richardson and Zaki (1954)** has widely been used since it is simple and in good agreement with experimental data:

$$\frac{U_l}{U_i} = \varepsilon_1^n \quad (5)$$

Where  $n$  is the Richardson–Zaki index, and can be respectively determined from the following relations:

$$n = 4.4 + 18\left(\frac{d_p}{D}\right) \text{Re}_t^{-0.1} \quad 1 < \text{Re}_t < 200 \quad (6)$$

$$n = 4.4 \text{Re}_t^{-0.1} \quad 200 < \text{Re}_t < 500 \quad (7)$$

$$n = 2.4 \quad \text{Re}_t > 500 \quad (8)$$

And  $U_i$  is the superficial fluid velocity at  $\varepsilon_1 = 1$ , which can be calculated from the following equation:

$$\log U_i = \log U_{pt} - \frac{d_p}{D} \quad (9)$$

Where  $U_{pt}$  is the particle terminal velocity

### 2.1.2. Gas holdup:

Gas hold  $\varepsilon_g$  characteristic has been also investigated by **Fan et al. (1982)**. They plotted gas hold-up against superficial gas velocity  $U_{go}$  as shown in fig3 and axial variation of gas hold up in fig4. It is observed that in the inverse bubbling fluidizing bed regime the liquid flow rate has negligible effect on  $\varepsilon_g$ . In contrast, in the conventional cocurrent up-flow gas-liquid-solid fluidized bed using large particles, the gas hold-up decreases with an increase in the liquid flow rate. Furthermore, in the inverse slugging fluidized bed regime, the gas hold-up increases with an increase in the liquid flow rate (**Fan et al., 1982; Lung et al., 1982; Krishnaiah et al., 1993**).

**Zhang et al. (1998)** have shown some effects of gas hold up on the hydrodynamics of IFB. They found that increased gas hold-up in the upper region of the bed eventually becomes sufficient to reduce the effective fluid (gas-liquid emulsion) density immediately below the particles to a point where the bed expands downwards into a fluidized state.

**Han et al. (2000)** investigated effects of the superficial gas velocity and particle loading on the gas holdup in the riser. They concluded that for any particle loading, the gas holdup in the riser increases with increasing superficial gas velocities. For a given particle loading, the increase of the gas holdup in the riser becomes less steep with the increase in the superficial gas velocity at high gas velocity. This may be explained by the fact that gas bubbles tend to coalesce with the increase in the superficial gas velocity.

The experimental method of measuring gas holdups has been illustrated as below.

$$H_1 \rho_l g = H_0 + (\varepsilon_l \rho_l + \varepsilon_g \rho_g) g + H_2 \rho_l \quad (10)$$

Since  $\rho_l \gg \rho_g$  and  $\varepsilon_g + \varepsilon_l = 1$  the following equation can be obtained:

$$\varepsilon_g = \frac{\Delta H}{H_0} \quad (11)$$

where  $\Delta H$  represents the level difference in the inverse U-type manometer and  $H_0$  the distance between two measured points.

**Omar et al. (2005)** reported that the volumetric gas–liquid mass transfer coefficient ( $k_{La}$ ) is independent of the solid hold-up but adversely depends on gas hold-up.

Their observation for the axial variation of gas holdup along the length of the column as shown in fig. 4 indicates that the gas holdup is almost uniform, within the range of liquid and gas velocities studied i.e value of velocity range to be given. It has also observed that the gas holdup is relatively small varying between 0.5% and 2% under the experimental conditions (**Krishna et al.,2007**).

The gas holdup is calculated using following equation (**Jena et al.1987**)

$$\varepsilon_g = 5.53 Fr_g^{0.4135} Re_L^{-0.1808} H_r^{0.0597} d_r^{0.0873} \quad (12)$$

### 2.1.3. Solid holdup:

For using a laboratory scale inverse turbulent bed reactor **Omar et al. (2005)** studied the solid hold-up for a gas –liquid solid system as follows:

$$\varepsilon_s = \frac{M}{AH\rho} \quad (13)$$

Where M is the mass of solid (kg), A is the cross-sectional area of the column (m<sup>2</sup>), H the bed height (m), and  $\rho$  is the solid density (kgm<sup>-3</sup>).

### 2.1.4. Liquid holdup:

Some researcher **Han et al. (2000)**,**Renganathan et al. (2005)**,**Krishna et al. (2007)** studied the variation of average phase holdups with liquid velocity at constant gas velocity. It is observed that at constant gas velocity, the liquid holdup increases and solid hold up decreases with increasing liquid velocity due to the expansion of the bed under fluidized bed condition. However, the gas hold up is almost constant with increase in liquid velocity.

The liquid holdup is calculated from the following equation.

$$\varepsilon_g + \varepsilon_l + \varepsilon_s = 1 \quad (14)$$

### 2.1.5. Minimum fluidization velocity:

The minimum fluidization velocity  $u_{mf}$  is an important hydrodynamic parameter involved in the design of this type of system. It is defined as the lowest superficial velocity at which the downward weight of the particles the drag force due to downward flow of the liquid just counters the upward buoyancy force of the solid particles, i.e., the net upward force is equal to the net downward force. Actual bed pressure drop,  $\Delta P$ , has been measured for a particular liquid velocity,  $u_f$ , by subtracting the solid-free pressure drop,  $\Delta P_o$ , due to liquid flow at identical liquid velocity,  $u_f$ , from the observed pressure drop,  $\Delta P_a$ , with solids present. Hence,

$$\Delta P = \Delta P_a - \Delta P_o \quad (15)$$

It is observed that as the bed weight increases the pressure drop increases but the minimum inverse fluidization velocity is almost constant and is independent of bed weight. Basically two factors affecting the minimum inverse fluidization velocity namely the particle density and size. For each gas velocity the minimum liquid fluidization velocity corresponds to the velocity of liquid at which the pressure gradient within the bed is minimum (**Ibrahim et al. 1996**). Hence, the minimum liquid fluidization velocity is obtained from a plot of pressure gradient vs. liquid velocity at a constant gas velocity (**Krishna et al., 2007**). As the gas velocity is increased, the liquid velocity required for maintaining the bed under minimum fluidization conditions is reduced as observed by several other authors (**Buffiere and Moletta, 1998; Ibrahim et al., 1996; Lee et al., 2000; Legile et al., 1992; Renganathan & Krishnaiah, 2004**).

## 2.2 Chemical oxygen demand:

In environmental chemistry, the **chemical oxygen demand (COD)** test is commonly used to indirectly measure the amount of organic compounds in water. Most applications of COD determine the amount of organic pollutants found in surface water (e.g. lakes and rivers) or wastewater, making COD a useful measure of water quality. It is expressed in milligrams per liter (mg/L), which indicates the mass of oxygen consumed per liter of solution. The (COD) is a measurement of the amount of material that can be oxidized in the presence of a strong chemical oxidizing agent. Since test can be performed rapidly it is often used as a rough approximation of the pollution level of concerned wastewater. It is calculated from the following formula.

$$\text{COD in mg/l} = \frac{(A - B) \times 0.025 \times 1000 \times 8}{20}$$

(16)

Where A = ml FAS used for blank

B = ml. FAS used for sample

**2.3 Biochemical oxygen demand:** The Biochemical oxygen demand (BOD) is a measure of the oxygen utilised by microorganisms during biological oxidation of organic matter contained in the liquid waste under specified experimental condition. The working formula is as follows.

$$BOD \text{ at } 20^\circ \text{C of the sample} = \left[ \frac{(D_0 - D_5) \times \text{vol. of sample}}{\text{ml. of sample}} \right] - (C_0 - C_5)$$

(17)

Where the initial D.O. of diluted sample =  $D_0$

D.O. at the end of 5 days for the diluted sample =  $D_5$

initial D.O. of distilled water(blank) =  $C_0$

D.O. at the end of 5 days for the distilled water (blank) =  $C_5$

D.O. depletion of dilution water =  $C_0 - C_5$

D.O. depletion of dilution sample =  $D_0 - D_5$

D.O. depletion due to microbes =  $(D_0 - D_5) - (C_0 - C_5)$

Similarly total suspended solid is calculated from the below mentioned formula.

$$TSS = \frac{\text{Final wt. of Filter paper} - \text{Initial wt. of filter paper} \times 1000 \times 1000}{\text{ml. of sample}}$$

(18)

## 2.4. Previous work on IFBB

**Sokol & korpál (2006)** investigated in the inverse fluidized bed biofilm reactor (IFBBR) in which polypropylene particles of density  $910 \text{ kg/m}^3$  were fluidized by an upward co-current flow of gas and liquid. Measurements of chemical oxygen demand (COD) versus residence time  $t$  are performed for various ratios of settled bed volume to bioreactor volume ( $V_b/VR$ ) and air velocities  $u$  to determine the optimal operating parameters for a reactor, that is, the values of ( $V_b/VR$ ),  $u$  and  $t$  for which the largest reduction in COD occurred. The biomass loading in a reactor depended on the ratio ( $V_b/VR$ ) and an air velocity  $u$ . In the cultures cultivated after change in ( $V_b/VR$ ) at a set  $u$ , the steady-state mass of cells grown on the particles was achieved after approximately 3 days of operation. With change in  $u$  at a set ( $V_b/VR$ ), the new steady-state biomass loading occurred after cultivation for about 2 days.

**Chen et al. (2009)** analyzed Bed expansion behavior and sensitivity analysis for super-high-rate anaerobic bioreactor (SAB) based on bed expansion ratio ( $E$ ), maximum bed sludge content ( $V_{p_{\max}}$ ), and maximum bed contact time between sludge and liquid ( $\tau_{\max}$ ). Bed expansion behavior models are established under bed unfluidization, fluidization, and transportation states. Under unfluidization state,  $E$  was 0,  $V_{p_{\max}}$  was 4867 ml, and  $\tau_{\max}$  was 844–3800s. Under fluidization state,  $E$ ,  $V_{p_{\max}}$ , and  $\tau_{\max}$  were 5.28%–255.69%, 1368–4559 ml, and 104–732 s, respectively. Under transportation state, washout of granular sludge occurred and destabilized the SAB. During stable running of SAB under fluidization state,  $E$  correlated positively with superficial gas and liquid velocities ( $u_g$  and  $u_l$ ), while  $V_{p_{\max}}$  and  $\tau_{\max}$  correlated negatively. For  $E$  and  $V_{p_{\max}}$ , the sensitivities of  $u_g$  and  $u_l$  were close to each other, while for  $\tau_{\max}$ , the sensitivity of  $u_l$  was greater than that of  $u_g$ . The prediction from these models is a close match to the experimental data.

**Sowmeyan & Swaminathan (2007)** worked to evaluate the feasibility of an inverse fluidized bed reactor for the anaerobic digestion of distillery effluent, with a carrier material that allows low energy requirements for fluidization, providing also a good surface for biomass attachment and development. Inverse fluidization particles having specific gravity less than one are carried out in the reactor. The carrier particles chosen for this study was perlite having specific surface area of  $7.010 \text{ m}^2/\text{g}$  and low energy requirements for fluidization. Before starting up the reactor,

physical properties of the carrier material are determined. One millimeter diameter perlite particle is found to have a wet specific density of 295 kg/m<sup>3</sup>. It was used for the treatment of distillery waste and performance studies are carried out for 65 days. Once the down flow anaerobic fluidized bed system reached the steady state, the organic load is increased step wise by reducing hydraulic retention time (HRT) from 2 days to 0.19 day, while maintaining the constant feed of chemical oxygen demand (COD) concentration. Most particles have been covered with a thin biofilm of uniform thickness. This system achieved 84% COD removal at an organic loading rate (OLR) of 35 kg COD/m<sup>3</sup>/day.

**Gomez et al. (2006)** immobilized derivatives of soybean peroxidase in a laboratory scale fluidized bed reactor to study their viability for use in phenol removal. The influence of the different operational variables on the process is also studied a reactor model based on the experimental results that predicts the system's behavior both in steady and transient state is developed. The model considers the fluidized bed reactor as a plug flow reactor in series with an ideal mixer and follows a kinetic law based on the observed external mass transfer resistances in order to work out the process rate.

**Bendict et al. (2006)** conducted experiments using 6 mm diameter spherical particles of low-density polyethylene (LDPE) and polypropylene (PP) with water and aqueous solutions of Carboxy methyl cellulose (CMC). It was found that the minimum fluidization velocity,  $U_{mf}$  decreased with an increase in CMC concentration and solid density. A dimensionless correlation was proposed for the prediction of bed height at fully fluidized conditions.

As in classical fluidization the pressure drop increased with increase in liquid flow rate till the condition of onset of fluidization is reached which represents packed bed. On further increase the pressure drop remains almost constant as the resistance for the liquid decreases significantly.

**Vijaya Lakshmi et al. (2005)** studied the hydrodynamic characteristics (bed expansion and pressure drop) of low-density polyethylene (LDPE) and polypropylene (PP) (4, 6 and 8 mm) in a liquid-solid inverse fluidized bed reactor as a function of particle diameter, liquid viscosity and density. The bed expansion and pressure drop data are used to determine the minimum fluidization velocity,  $U_{mf}$  and friction factor. It was found that the  $U_{mf}$  increased with an increase in the particle diameter and a decrease in solid density and was independent of initial bed height (solid loading). In addition, the  $U_{mf}$  decreased with an increase in the CMC concentration. The

friction factor Reynolds number plot is found similar to that of classical fluidization. Dimensionless equations were proposed for the prediction of the friction factor and the  $U_{mf}$ .

**Fuentes et al. (2007)** analyzed the adequacy of some hypotheses assumed in the literature for modeling mass transfer phenomena and hydrodynamics in bioreactors. Four different hydrodynamic models are investigated to simulate the dynamic behavior of an anaerobic Fluidized bed reactor (AFBR). A total developed flow condition and the assumption of an incipient gas phase are some of the evaluated hypotheses. All models simultaneously compute the dynamics of the phases and their components, including the effect of the bio film growth in the fluidization characteristics.

**Allia et al. (2006)** investigated biological treatment in two different systems namely: aerated closed system and three phase fluidized bed reactors for removal of hydrocarbons from refinery wastewaters. This typical bioreactor allows a good removal rate of pollutants. According to **Allia et al. (2006)** the elimination of hydrocarbons in the three-phase fluidized bed bioreactor is lower than that of the aerated agitated closed bioreactor. They observed the elimination in aerated closed was around 100%, while in three phase fluidized bed reactors elimination was between 87.77 - 95%.

**Sokol et al. (2005)** investigated the biological wastewater treatment in the inverse fluidized bed reactor (IFBR) in which polypropylene particles of density  $910 \text{ kg/m}^3$  was fluidized by an upward flow of gas. Measurements of chemical oxygen demand (COD) versus residence time  $t$  are carried out for various ratios of settled bed volume to reactor volume ( $V_b/VR$ ) and air velocities  $u_g$ . The largest COD removal is attained when the reactor was operated at the ratio  $(V_b/VR)_m = 0.55$  and an air velocity  $U_{gm} = 0.024 \text{ m/s}$ . Under these conditions, the value of COD was practically at steady state for around greater than 30 h of time duration. Thus, these values of  $(V_b/VR)_m$ ,  $U_{gm}$  and  $t$  can be considered as the optimal operating parameters for a reactor when used in treatment of industrial wastewaters. As per their observation a decrease in COD from 36,650 to 1950 mg/l, i.e. a 95% COD reduction, is achieved when the reactor is optimally controlled at  $(V_b/VR)_m = 0.55$ ,  $u_g = 0.024 \text{ m/s}$  and  $t = 30 \text{ h}$ . The pH is controlled in the range 6.5–7.0 and the temperature was maintained at 28–30°C.

**Garcia et al. (1998)** applied down flow (or inverse) fluidization technology for the anaerobic digestion of red wine distillery wastewater. The carrier employed is ground perlite, an expanded



volcanic rock. Before starting-up the reactor, physical and fluidization properties of the carrier material were determined.. Once the down-flow anaerobic fluidized bed system reached the steady-state, organic load is increased step- wise by reducing HRT, from 3.3-1.3 days, while maintaining constant the feed TOC concentration. The system achieved 85% TOC removal, at an organic loading rate of 4.5 kg TOC m<sup>3</sup> d<sup>-1</sup>. It is found that the main advantages of this system are: low energy requirement, because of the low fluidization velocities required; there is no need of a settling device, because solids accumulate at the bottom of the reactor so they can be easily drawn out, and particles with high-biomass content, whose specific density have become larger than 1000 kg m<sup>-3</sup> can be easily recovered.

The anaerobic fluidized bed reactor utilizes small, fluidized media particles to induce extensive cell immobilization thereby achieving a high reactor bio- mass hold-up and a long mean cell residence time.

The organic loading rate (OLR) and the carbon removal yield (Y) were calculated by **Garcia et al. (1998)** as:

$$\text{OLR} = (Q_{\text{in}}) (C_{\text{in}})/V_{\text{exp}} \quad (19)$$

$$Y = (C_{\text{in}} - C_{\text{out}}) / C_{\text{in}} \quad (20)$$

According to work that has been done by **Arnaiz et al.(2002)** the ITB (inverse turbulent bed) bed reactor appeared to be a good option for anaerobic treatment of high strength wastewater, particularly for the treatment of wine distillery wastewater. The system attained high organic loading rate (OLR) with good chemical oxygen demand (COD) removal rates and it exhibited a good stability to the variations in OLR and HRT (hydraulic retention time). They found that the main advantages of this system are: low energy requirement because of the low fluidization velocities required; there is no need of a settling device, because solids accumulate at the bottom of the reactor, so they can be easily drawn out and particles with high-biomass content can be easily recovered. They also examined whether changes in liquid coalescing properties caused by minute concentrations of additives can greatly affect the hydrodynamic properties of a three-phase inverse fluidized bed.

Success of the design and the operation of a inverse fluidised bed bioreactor (IFBB) depends a great deal on the accurate prediction of the fundamental properties of the system, especially, the hydrodynamics in the reactor as well as the physical and chemical properties of

the feed. Although, IFBB is simple to construct and easy to operate, its scale up poses a significant challenge due to the complex interaction among many parameters. The complexity of the interdependence of the hydrodynamic aspects and the intrinsic kinetic ones has resulted in the development of different mathematical models. However, none of the models explicitly describes the bed characteristics to enable accurate scale up. In the present work some attempts have been made to identify and quantify the design parameters, however, wide scale application of a fluidised bed bioreactor still poses a challenge due to the fact that the parameters are waste specific. Three main system parameters such as oxygen flow rate, sample flow rate and bed volume and their effects were analysed.

One of the principal requirements for a bioreactor is the ability of the micro-organisms to grow on the support particle and remain embedded for significant biodegradation to take place. The microbial growth rate is so crucial for bioreactor performance that a lot of attention has been given to this, owing to the fact that bed turbulence and the nature of support particle appreciably affect microbial attachment. Considering the nature of the waste, it has been found necessary to adjust nutrient content and pH to enable initial microbial growth. Gas flow rate affects phase mixing and gas hold ups, which are important parameters that influence oxygen mass transfer. The survival as well as the activity of the aerobic micro-organisms depends on the amount of oxygen dissolved. A well mixed medium will give rise to a homogeneous bed that promotes interfacial mass transfer, and this will make oxygen available to the micro-organisms.

In the present work some attempts have been made to identify and quantify the design parameters, however, wide scale application of a fluidised bed bioreactor still poses a challenge due to the fact that the parameters are waste specific. Three main system parameters such as oxygen flow rate, sample flow rate and bed volume and their effects were analysed. Then these parameters were optimised in which maximum COD removal occurred from sample industrial effluents.

## **2.5. Factorial design**

In statistics, a full factorial experiment is an experiment whose design consists of two or more factors, each with discrete possible values or "levels", and whose experimental units take on all possible combinations of these levels across all such factors. A full factorial design may

also be called a fully crossed design. Such an experiment allows studying the effect of each factor on the response variable, as well as the effects of interactions between factors on the response variable.

For the vast majority of factorial experiments, each factor has only two levels. For example, with two factors each taking two levels, a factorial experiment would have four treatment combinations in total, and is usually called a  $2^2$  factorial design.

If the number of combinations in a full factorial design is too high to be logistically feasible, a fractional factorial design may be done, in which some of the possible combinations (usually at least half) are omitted.

The simplest factorial experiment contains two levels for each of two factors. This experiment is an example of a  $2^2$  factorial experiment, so named because it considers two levels (the base) for each of two factors (the power or superscript).

Designs can involve many independent variables. As a further example, the effects of three input variables can be evaluated in eight experimental conditions shown as the corners of a cube.

This can be conducted with or without replication, depending on its intended purpose and available resources. It will provide the effects of the three independent variables on the dependent variable and possible interactions.

To save space, the points in a two-level factorial experiment are often abbreviated with strings of plus and minus signs. The strings have as many symbols as factors, and their values dictate the level of each factor: conventionally, - for the first (or low) level, and + for the second (or high) level. The points in this experiment can thus be represented as --, +-, -+, and ++.

The factorial points can also be abbreviated by (1), a, b, and ab, where the presence of a letter indicates that the specified factor is at its high (or second) level and the absence of a letter indicates that the specified factor is at its low (or first) level (for example, "a" indicates that factor A is on its high setting, while all other factors are at their low (or first) setting). (1) is used to indicate that all factors are at their lowest (or first) values (**W. Volk, 1969**).

**Implementation**

For more than two factors, a  $2^k$  factorial experiment can be usually recursively designed from a  $2^{k-1}$  factorial experiment by replicating the  $2^{k-1}$  experiment, assigning the first replicate to the first (or low) level of the new factor, and the second replicate to the second (or high) level. This framework can be generalized to, e.g., designing three replicates for three level factors, etc.

A factorial experiment allows for estimation of experimental error in two ways. The experiment can be replicated, or the sparsity-of-effects principle can often be exploited. Replication is more common for small experiments and is a very reliable way of assessing experimental error. When the number of factors is large (typically more than about 5 factors, but this does vary by application), replication of the design can become operationally difficult. In these cases, it is common to only run a single replicate of the design, and to assume that factor interactions of more than a certain order (say, between three or more factors) are negligible. Under this assumption, estimates of such high order interactions are estimates of an exact zero, thus really an estimate of experimental error.

When there are many factors, many experimental runs will be necessary, even without replication. For example, experimenting with 10 factors at two levels each produces  $2^{10}=1024$  combinations. At some point this becomes infeasible due to high cost or insufficient resources. In this case, fractional factorial designs may be used.

As with any statistical experiment, the experimental runs in a factorial experiment should be randomized to reduce the impact that bias could have on the experimental results. In practice, this can be a large operational challenge.

Factorial experiments can be used when there are more than two levels of each factor. However, the number of experimental runs required for three-level (or more) factorial designs will be considerably greater than for their two-level counterparts. Factorial designs are therefore less attractive if a researcher wishes to consider more than two levels.

## **CHAPTER-3**

### **EXPERIMENTAL WORK**

The setup of Inverse fluidized bed is operated in different modes. In 2-phase IFB, the solids are fluidized using only liquid (no gas phase) flowing from the top. The 3-phase IFB can be operated with dispersed gas phase sent from the bottom of the column through the liquid phase which can be either in batch or continuous mode. In 3-phase IFB with liquid in batch mode, the solid particles are maintained in a fluidized condition by means of gas flow only with no net liquid flow. In the continuous mode of operation, both liquid and gas phases contribute to the downward fluidization of the particles.

### 3.1 Experimental Set up

Fig.1 shows the experimental setup. The column was made of Perspex and had the dimension of 100 mm internal diameter with a maximum height of 1240 mm and a wall thickness of 3 mm. The column consisted of three sections, namely,

- Conical liquid distribution section:

This section consists of a cone with angle of  $30^\circ$  whose large base dia is same as the dia of the column i.e. 10 cm and small base diameter is 3 cm. at the top of the cone a vent or exit is provided for the inlet gas. The distributor is also kept at the top of the column. ball valves are there to control the incoming water low rate.

- Test section:

The test section is made up off column of height 100 cm. 10 number of pressure tappings are provided at equal distance of the column. The pressure tappings are connected with manometers with help of pipes.

- Conical liquid discharge section.:

This section consists exit outlet for the water, at the bottom of the column another distributor is given to prevent the particles from escaping the bed. This distributor also works as sparger of air. A non returning control valve is there to let the air in.

- Five number of manometers(1 mtr) are there to measure the bed pressure drop. These manometers are filled with carbon tetra chloride.



Fig.1: Setup of inverse fluidized bed.

The conical head liquid distributor located at the top of the column was designed in such a way that uniform liquid distribution across the column cross section could be ensured. A wire gauge was provided at the bottom of the column, after the distributor plate just above the liquid discharge section to prevent elutriation of the particles into the liquid exit. A wire mesh was also provided at the top of the column to prevent the particles to escape out from bed. Liquid was pumped to the top of the column through the calibrated rotameters (range: 0 - 100 LPM). The column could be loaded with solid particles from the top of the column. In this work water was used as the fluidizing liquid. The pressure taps were evenly spaced at 100 mm intervals on the wall of the test section and connected to carbon tetrachloride manometers. The liquid discharge section connects a pipe to the reservoir transfer the liquid to the tank so that it is re-circulated. A control valve is also provided in the discharge line to adjust the flow rate.

**3.2. Parts of Setup :**

1. The fluidised bed consists of a perspex column with a height of 1024 mm and diameter of 100 mm. The thickness of the column is 3 mm.
2. To pump the water a Centrifugal Pump is used. (Power=0.5 HP, Head=14 ft.)
3. Calibrated water rotameter of capacity 0-100 LPM is used.
4. Calibrated air rotameter measuring flowrate (0-1000 lph) is used.
5. Five numbers of manometers with standard length of 1.0 m are used.
6. Syntax water reservoir - capacity: 1000 Liters.
8. Circular pitch distributed plates with different pitch diameters are used.
9. Two Conical heads with apex angle of  $60^\circ$  are used at top and bottom of the column. (Inner base diameter = 100 mm, height = 30 cm).

**3.3. Experimental procedure:**

1. The two rotameters were calibrated by comparing the reading with the measured flow rate.
2. In a typical experiment, the column was loaded with solid particles of a particular size and density of the required bed height.
3. Water was fed to the column at a known flow rate, the system was allowed to attain steady state by adjustment of inlet and discharge flow rate.
4. The manometers were filled with carbon tetrachloride and the pressure drop across the test section was noted from the manometers.
5. Water flow rate was increased gradually in steps till the bed was completely fluidized. Depending on the flow rate of liquid through the column, only a packed bed, or a partially packed and fluidized bed were encountered. These bed heights were measured by visual observation.
6. The pressure drop was plotted against the distance between the tappings along the entire column for the flow rate taken (3-15 LPM).
7. The velocity at which the entire bed just became fluidized was noted as the minimum fluidization velocity.



8. The physical properties of the particles and operating conditions are given in the experimental specifications.

### 3.4 Method for hydrodynamic studies:

Initially tap water was taken as the fluidising medium. Then various hydrodynamic behaviour were studied. The parameters like air flow rate, water flow rate, distributor size and static bed height. The effects of these parameters over bed pressure drop were analysed. Static bed height is varied keeping all three parameters constant. Similarly experiments were conducted by changing one parameter and all other three parameter constant.

## 3.5 Biological Treatment Of Waste Water

### 3.5.1 Methodology

Various hydrodynamic properties of inverse fluidized bed were studied using pond water as the continuous medium. It have reported that the largest values of air hold-up  $\varepsilon$ , and thus the largest interfacial area were obtained when a bioreactor with polypropylene particles was controlled at ratio  $(V_b/V_R)$  in the range 0.50–0.60. It is established that the optimal value of  $(V_b/V_R)$  for a bioreactor when used in treatment of refinery wastewater was equal to 0.55. Therefore, in this study experiments were conducted for the ratios  $(V_b/V_R)$  equal to 0.50, 0.55 and 0.60. This was to cover the searched range of  $(V_b/V_R)$  from 0.50 to 0.60 in step 0.05 which is sufficient accuracy for industrial practice.

### 3.5.2 Analysis of sample

The various physical as well as chemical properties were isolated such as density, pH, BOD, COD, TSS, TOC.

### 3.5.3. Measurement of COD (Chemical Oxygen Demand)

#### 3.5.3.1 Principle :

Most types of organic matters are oxidized by a boiling mixture of chromic and sulfuric acids. A sample is refluxed in strongly acid solution with a known excess of potassium dichromate. After

digestion, the remaining unreduced  $K_2Cr_2O_7$  is titrated with ferrous ammonium sulphate to determine the amount of  $K_2Cr_2O_7$  consumed and the oxidizable matter is calculate in terms of oxygen equivalent.

#### 3.5.3.2 Reagents :

##### (1) $K_2Cr_2O_7$ Solution :

12.259 gm of  $K_2Cr_2O_7$  is dissolved (previously dried at  $150^\circ C$  for 2 hour) in distilled water and diluted to 1000 ml.

##### (2) Conc. $H_2SO_4$

##### (3) Ferroin Indicator:

##### (4) Ferrous Ammonium Sulphate (FAS) :

98 gm  $Fe(NH_4)_2(SO_4)_2 \cdot 6H_2O$  is dissolved in distilled water. 20 ml conc.  $H_2SO_4$  was added and diluted to 1000 ml. Standardised as follows :

##### Standardisation :

10 ml standard  $K_2Cr_2O_7$  is diluted to about 100 ml, 30 ml conc.  $H_2SO_4$  was added ,cooled. 2 drops of ferroin indicator was added and titrated with FAS.

Molarity FAS = volume of  $K_2Cr_2O_7$  in ml X 0.25 / Volume of FAS used in ml

##### (5) Mercuric Sulphate Powder ( $HgSO_4$ )

#### 3.5.3.3 Procedure :

20 ml sample was taken in 500 ml flask .Then 10ml  $K_2Cr_2O_7$  was added. 30 ml conc.  $H_2SO_4$  was added very slowly and cautiously. Then 0.4 gm of Mercuric sulphate powder was added. It is kept over a magnetic hotplate at  $120^\circ C$ . The solution was cooled to room temperature. The solution was transfer to a 500 ml conical flask. The solution was diluted to twice its volume with distilled water. Titrated against FAS, using 2 to 3 drops of ferroin indicator. Take as the end point of the titration the first sharp color change from blue green to reddish brown that persists for 1 minute and longer. In the same manner a blank was titrated containing the reagents and volume of distilled water equal to that of sample.

### 3.5.4. Measurement of BOD (Biochemical oxygen demand)

#### 3.5.4.1 Principle:

The method consists of filling with sample, to overflowing, an airtight bottle of the specified size and incubating it at the specified temperature for 5 d. Dissolved oxygen is measured initially and

after incubation, and the BOD is computed from the difference between initial and final DO. Because the initial DO is determined shortly after the dilution is made, all oxygen uptake occurring after this measurement is included in the BOD measurement.

*Sampling and storage:* Samples for BOD analysis may degrade significantly during storage between collection and analysis, resulting in low BOD values. Minimize reduction of BOD by analyzing sample promptly or by cooling it to near-freezing temperature during storage. However, even at low temperature, keep holding time to a minimum. Warm chilled samples to  $20 \pm 3^{\circ}\text{C}$  before analysis.

#### 3.5.4.2 Reagents :

Prepare reagents in advance but discard if there is any sign of precipitation or biological growth in the stock bottles. Commercial equivalents of these reagents are acceptable and different stock concentrations may be used if doses are adjusted proportionally.

*a. Phosphate buffer solution:* 8.5 g  $\text{KH}_2\text{PO}_4$ , 21.75 g  $\text{K}_2\text{HPO}_4$ , 33.4 g  $\text{Na}_2\text{HPO}_4 \cdot 7\text{H}_2\text{O}$ , and 1.7 g  $\text{NH}_4\text{Cl}$  were dissolved in about 500 mL distilled water and dilute to 1 L. The pH should be 7.2 without further adjustment. Alternatively, 42.5 g  $\text{KH}_2\text{PO}_4$  or 54.3 g  $\text{K}_2\text{HPO}_4$  were dissolved in about 700 mL distilled water. Adjust pH to 7.2 with 30% NaOH and dilute to 1 L.

*b. Magnesium sulfate solution:* 22.5 g  $\text{MgSO}_4 \cdot 7\text{H}_2\text{O}$  was dissolved in distilled water and dilute to 1 L.

*c. Calcium chloride solution:* 27.5 g  $\text{CaCl}_2$  was dissolved in distilled water and dilute to 1 L.

*d. Ferric chloride solution:* 0.25 g  $\text{FeCl}_3 \cdot 6\text{H}_2\text{O}$  was dissolved in distilled water and dilute to 1 L.

*f. Sodium sulfite solution:* 1.575 g  $\text{Na}_2\text{SO}_3$  was dissolved in 1000 mL distilled water. This solution is not stable; should be prepared daily.

*g. Dilution water:* demineralized, distilled, tap, or natural water is used for making sample dilutions.

#### 3.5.4.3 Procedure:

The desired volume of the sample was placed in a 5 liter flask. 1 ml of phosphate buffer , 1 ml of magnesium sulphate solution, 1 ml of calcium chloride solution and 1 ml of ferric chloride solution was added for every liter of distilled water(dilution water).In the case of waste waters which are not expected to have sufficient bacterial population , add seed to the dilution water.

Generally, 2 ml of settled sewage is sufficient for 1000ml of dilution water. Highly acidic or alkaline sample are to be neutralized to pH of 7. 2 or 3 ml of sodium thiosulphate solution was added to destroy residual chlorine if any. The sample dilution was taken as follows: Strong wastes: 0.1,0.5, or 1%, Settled domestic sewage: 1,2.5 or 5%, Treated effluents: 5, 12.5 or 25%, River water :25 to100%.The sample was diluted with distilled water and the content was mixed well.Diluted sample was take in two BOD bottles. Immediately D.O. of a diluted wastewater and diluted water (distilled water) was found. The other two BOD bottles at 20<sup>0</sup> c for 5 or 3 days was incubated. They are tightly stoppered to prevent any air entry into bottles. D.O. content in the incubated bottles at the end of 5 or 3 days was determined.

### 3.5.5. Measurement of TSS

Procedure:

The initial weight of a clean dry beaker was taken. 50 ml water sample was taken in it. The initial weight of the filter paper was taken. Filter it and take in the beaker. The final weight of the filter paper was taken. Put it on hot plate for complete drying. The final weight of the beaker was taken.

### 3.5.6.Feed and microorganisms

Here the microorganism selected is the species *pseudomonas aeruginosa*. The species is selected for because of its phenol degrading properties. It is a common bacterium that can cause disease in animals, including humans. It is found in soil, water, skin flora, and most man-made environments throughout the world. It thrives not only in normal atmospheres, but also in hypoxic atmospheres, and has, thus, colonized many natural and artificial environments. It is a Gram-negative, aerobic, rod-shaped bacterium.

### 3.5.7. Inoculum preparation

The microbial species of *pseudomonas aeruginosa* is taken from the solidified slant culture. Then nutrient broth is prepared which is readymade available. 3.25 gm of nutrient was added to 250 ml of distilled water and the solution is checked for ph=7. It was autoclaved at 121<sup>0</sup> c for 20 min. & then it was cooled. Microbes are extracted from the mother culture by swapping method through inoculums loop and was mixed to the nutrient solution. Then it is kept at laminar flow

chamber at 30<sup>0</sup> c temp, 120 rpm and incubated for around 1 day. Again to make the volume upto 1 litre the procedure is repeated. This time the 250 ml. incubated solution is take as mother culture.

### 3.5.8. Biomass culturing

The particles and the growth medium were introduced into the bioreactor to give a ratio (Vb/VR)= 0.50. To start growth of the microorganisms on the particles, a batch culture was first initiated by introducing about 1liter of the inoculum into the bioreactor.

The air was supplied at the flow rate of  $2 \times 10^{-2} \text{m}^3 \text{s}^{-1}$  and this was found to be sufficient for biomass growth. Next, the air flow rate was set at such value to give the smallest air velocity applied for the ratio (Vb/VR)= 0.50 ( $u = 0.014 \text{ms}^{-1}$  in Fig 4) and the culturing was continued until constant biomass loading was achieved in a bioreactor. The occurrence of the steady state biomass loading was established by weighing the mass of cells grown on the support. The biomass was scraped from sample particles using a knife and dried at 105 °C for 1 h. It was considered that the steady state occurred when the weight of biomass in two consecutive samples differed by less than 5%.The constant biomass loading was attained ina bioreactor after culturing for approximately 3 days.

**Table 3.1.** Physical properties of some particles.

S No	Material	Diameter :d x 10 <sup>-3</sup> m	Density: $\rho_s \times 10^{-3}$ kg m <sup>-3</sup>
1	Polypropylene	4-6	(862-877)±25
2	Extendsphere	175X10 <sup>-6</sup>	690
3	Low density	3-4	914-934
4	Perlite	0.968	280
5	Polyethylene/ polypropylene	9.53-10	388-822
6	Polyethylene/ polypropylene	4.79-19.1	388-930
7	Polypropylene	9.53	822
	Polyethylene	6.53	930

**Table 3.2:** Scope of experiment for hydrodynamic studies

Sl.No.	Static bed height Hs(cm)	Distributor size Do(mm)	Water flow Rate $F_w \times 10^{-3}$ (m <sup>3</sup> /sec)	Air flow rate $F_a \times 10^{-3}$ (m <sup>3</sup> /sec)
1	12.5	3	1.84	555.556
2	15	3	1.84	555.556
3	17	3	1.84	555.556
4	10	2	1.84	555.556
5	10	4	1.84	555.556
6	10	5	1.84	555.556
7	10	3	2.00	555.556
8	10	3	2.50	555.556
9	10	3	3.30	555.556
10	10	3	3.80	555.556
11	10	3	4.70	555.556
12	10	3	6.20	555.556
13	10	3	6.70	555.556
14	10	3	1.84	555.556
15	10	3	1.84	555.556
16	10	3	1.84	694.444
17	10	3	1.84	833.333
18	10	3	1.84	111.111
19	10	3	1.84	138.888

**Table 3.3** Scope of experiment for COD removal efficiency

Sl. no.	Static bed height Hs(cm)	water flow rate Fw(lph)	oxygen flow rate Fa(m <sup>3</sup> /sec)
1	50	40	80
2	55	40	80
3	60	40	80
4	55	17	80
5	55	23	80
6	55	29	80
7	55	40	80
8	55	50	80
9	55	40	40
10	55	40	60
11	55	40	80
12	55	40	100
13	45	40	80

## **CHAPTER-4**

## **RESULTS AND DISCUSSIONS**



For all designing approaches, biochemical transformations are assumed to occur only in the fluidized bed zone but not in the free-support material zone. No mass transfer limitations in the biofilm and liquid film are assumed. The substrate concentration has the same value throughout the biofilm. Homogeneous biofilm distribution on the support particles, constant density and diameter of the support particles, constant wet biofilm density and spherical geometry are assumed for the bioparticle model. The number of support particles (i.e. the number of particles) is assumed constant and these are homogeneously distributed within the entire reactor.

#### 4.1. Hydrodynamic studies

If the entire bed is fluidized, the concentration of solids is not uniform along the axis of the bed. High concentration of solids is observed near the liquid distributor. For further increase in the velocity, the solid holdup becomes uniform throughout the bed. The effects of different system parameters on pressure drop were studied

##### 4.1.1 Results:

The effect of different system parameters on pressure drop viz. air flow rate, water flow rate, static bed height, distributor size were studied.

A correlation is developed using dimensional analysis for pressure drop as follows.

$$\Delta P = 9076.1 \times \left[ (H_s)^{0.194} (D_o)^{0.146} (F_w)^{0.281} (F_a)^{0.206} \right] \quad (15)$$

The effects were also studied using statistical analysis (**2<sup>4</sup> Factorial Design**). A correlation thus formulated for pressure drop is as follows.

$$\begin{aligned} \Delta P = & 2284.23 - 108.77H_s - 210.18D_o - 218.364H_s.D_o - 422.82F_w + 216.72H_s.F_w - \\ & 108.77D_o.F_w + 166.02H_s.D_o.F_w - 576.58F_a + 203.64H_s.F_a + 327.95D_o.F_a + \\ & 169.29H_s.D_o.F_a + 723.79F_w.F_a - 154.57H_s.F_w.F_a + 25.35D_o.F_w.F_a - \\ & 215.09H_s.D_o.F_w.F_a \end{aligned} \quad (16)$$

##### 4.1.2 Discussions:

It is observed that the bed expands with the increase in the liquid velocity. It is further observed that higher static bed height expands less in comparison with the lower static bed height. This may be due to more amount of solids in the bed with the higher static bed height for which liquid velocity might not be sufficient to cause more expansion.

The bed height remains unaffected (fixed) up to a certain liquid flow rate which corresponds to static condition or packed bed behavior. After the threshold point i.e. minimum fluidization condition the bed height varies linearly with the liquid flow rates. Effects of fluidization velocity on bed height and void fraction have been reported (Fig.2 & Fig.3). Comparison among different static bed heights indicates that lower static bed heights gives better expansion. Also the void fraction for lower static bed height is larger than the void fraction for higher static bed heights.

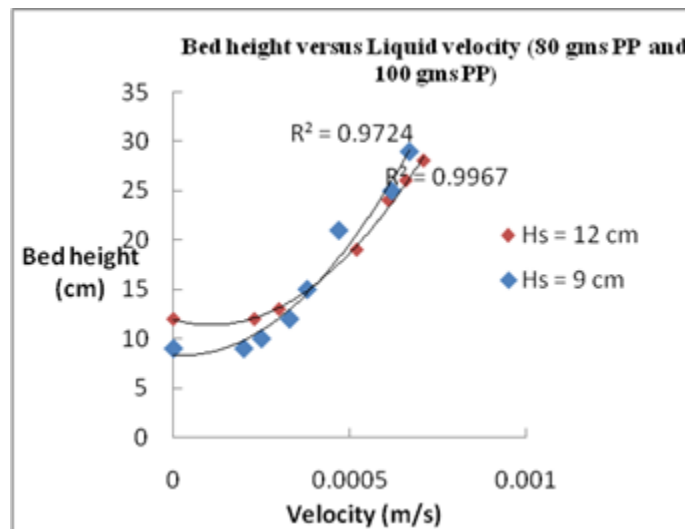


**Fig 2.** - Bed height versus liquid velocity for different bed weight.

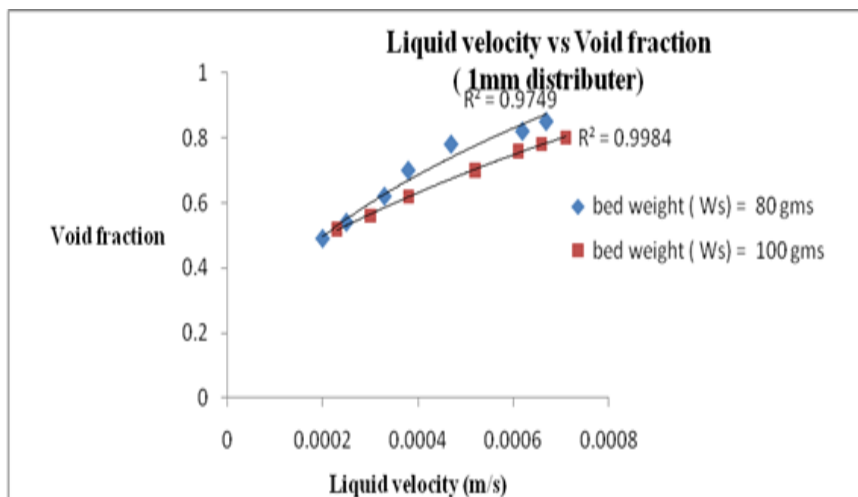


**Fig 3.** Liquid velocity versus void fraction.

Pressure drop profile ( $\Delta P$  vs.  $V$ ) against the velocity of liquid at different positions of the column are observed through different manometers have been shown in Fig-4 and 5 for two and three phase systems respectively. It is observed that at a particular liquid velocity the bed pressure drop increases with increase in bed height.

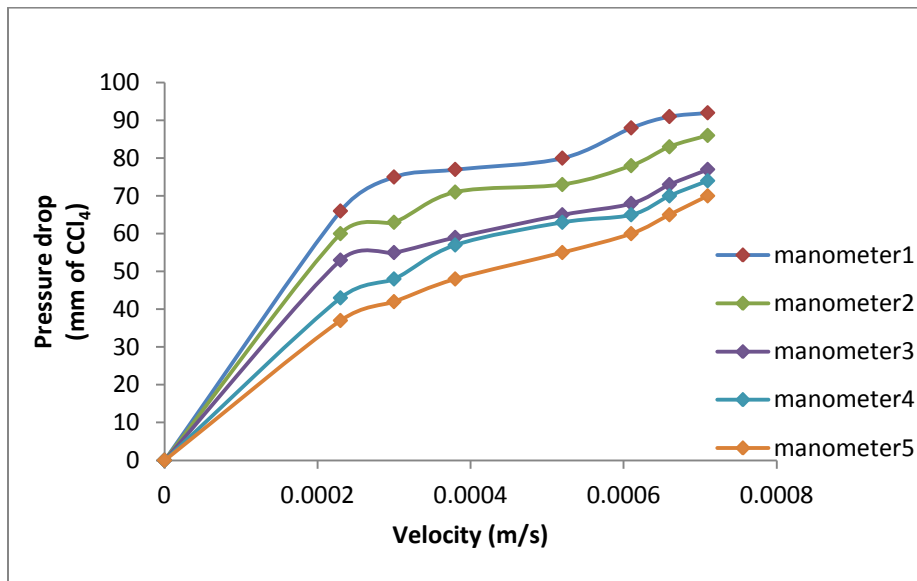


**Fig 4 :** Pressure drop profile against liquid velocity for static bed height of 12cm

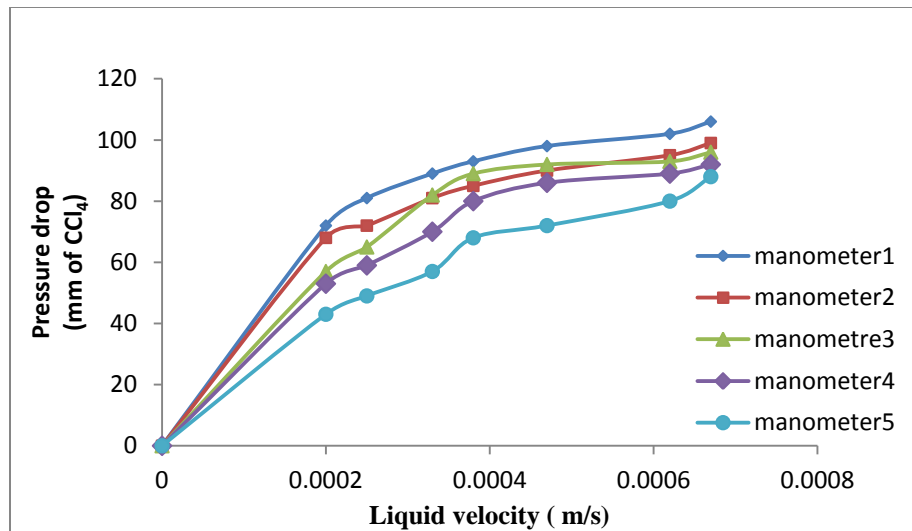


**Fig 5:** Pressure drop versus liquid velocity for bed weight 100 gms.

Initially tap water is taken as the continuous phase for carrying out in the inverse fluidised bed. The various hydrodynamics properties of water are studied. Initially the liquid flow rate was maintained constant at 30 lpm and the air flow was varied which was allowed to flow through the bottom of the inverse fluidised bed. Variation of pressure drop with the bed height at different air flow rates is shown in Fig-6. It is observed that the pressure drop at any height increases with the air flow rate. Pressure drop was also observed to increase with the bed height at a particular air flow rate. Variation of bed pressure drop with the bed height at an interval of 10cm measured through different manometers against the air flow rate is shown in Fig-7.

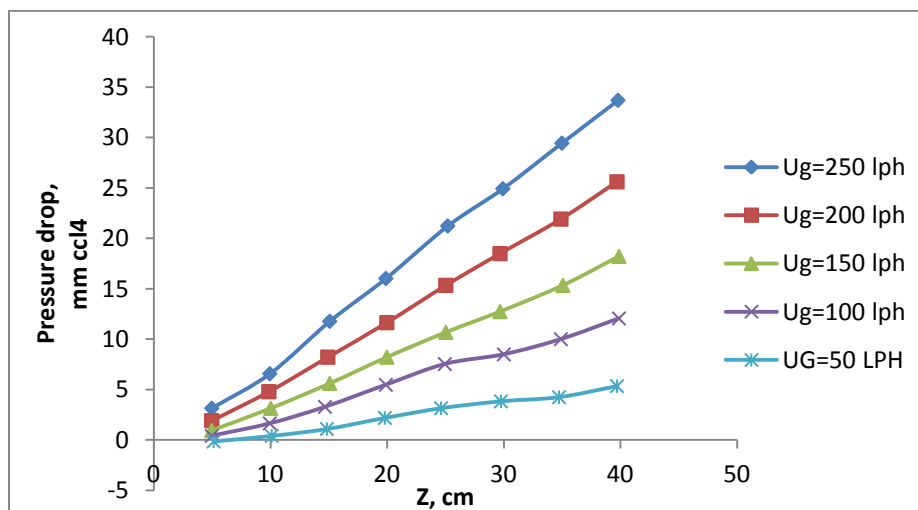


**Fig.6.** pressure variation versus bed height

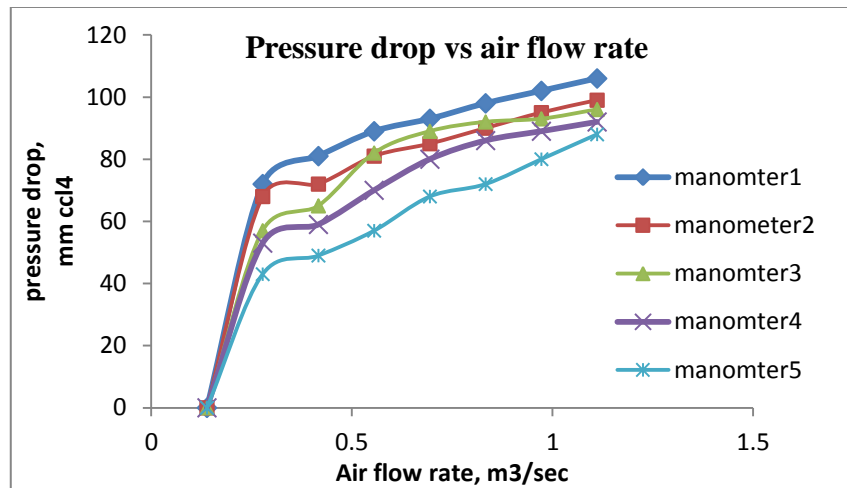


Fig.7.Pressure drop profile at various air flow rate

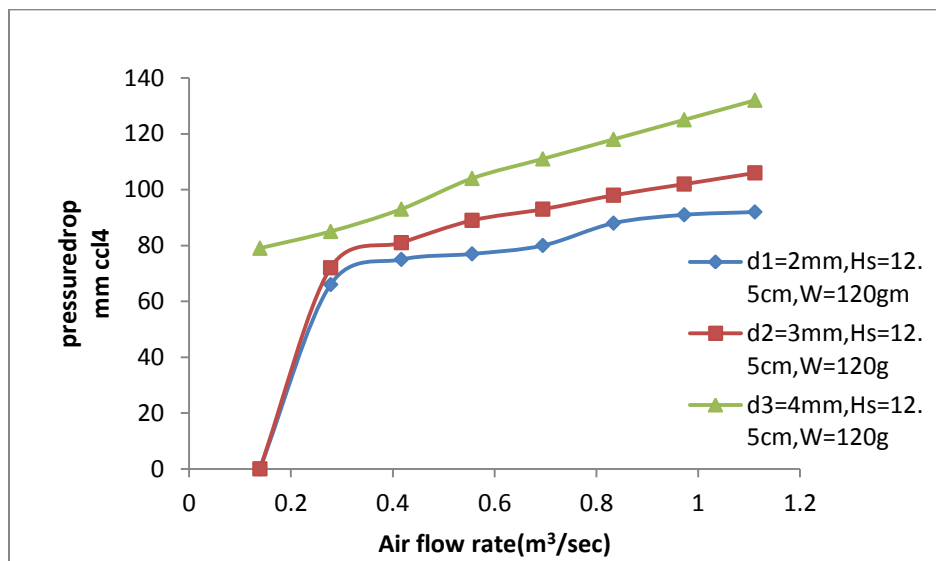


Fig.8.Comparison of pressure drop for different distributor for manometer 1

Bed pressure drop was also studied through Manometer-1 by varying the diameter of distributor orifices (Fig-8). It is observed that with increase in diameter of orifices, the pressure drop increases. Bed pressure drop was also studied through a particular manometer by varying the static bed heights (Fig.9). It is observed that with increase in static bed height and liquid velocity the pressure drop increases.

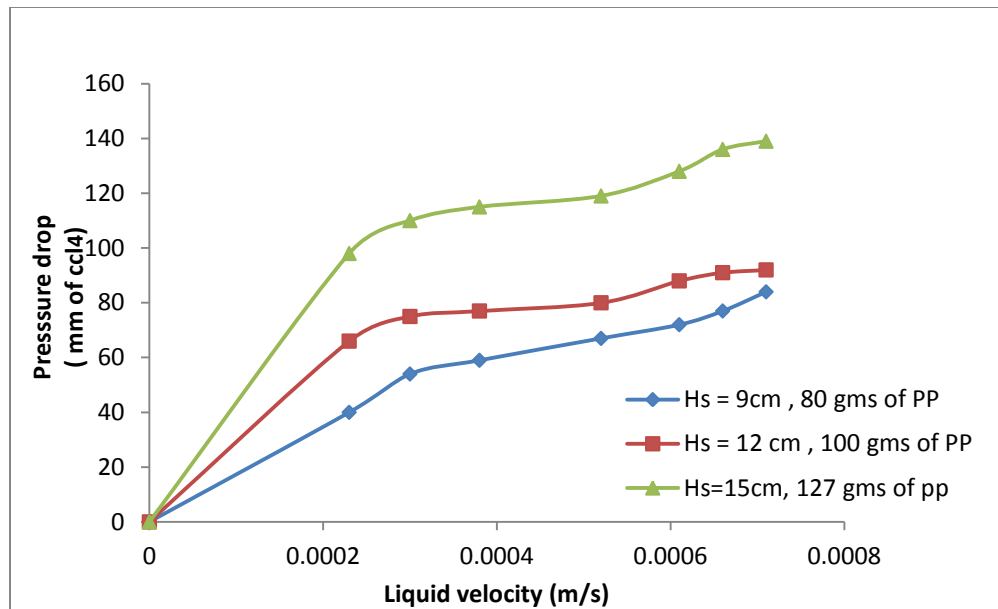


Fig.9.Comparison of pressure drop through manometer 1 for different static bed height

Then the inverse fluidised bed is also allowed to be run at constant gas flow rate by varying the liquid flow rate for which the pressure drop profile has been shown in Fig.-10.

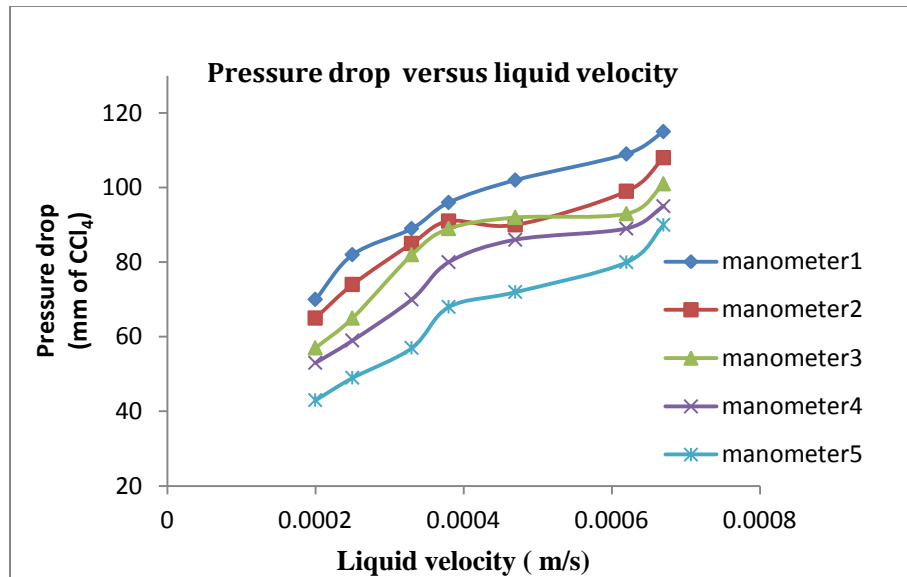


Fig.10. Pressure drop vs. liquid velocity

It is observed from the fig.10 that pressure drop is directly proportional to liquid velocity and also at a particular liquid velocity the bed pressure drop increases with increase in bed height as observed with different manometers connected at different locations of the bed.

Correlation plot for the bed pressure drop against the system parameters is shown in Fig.-11.

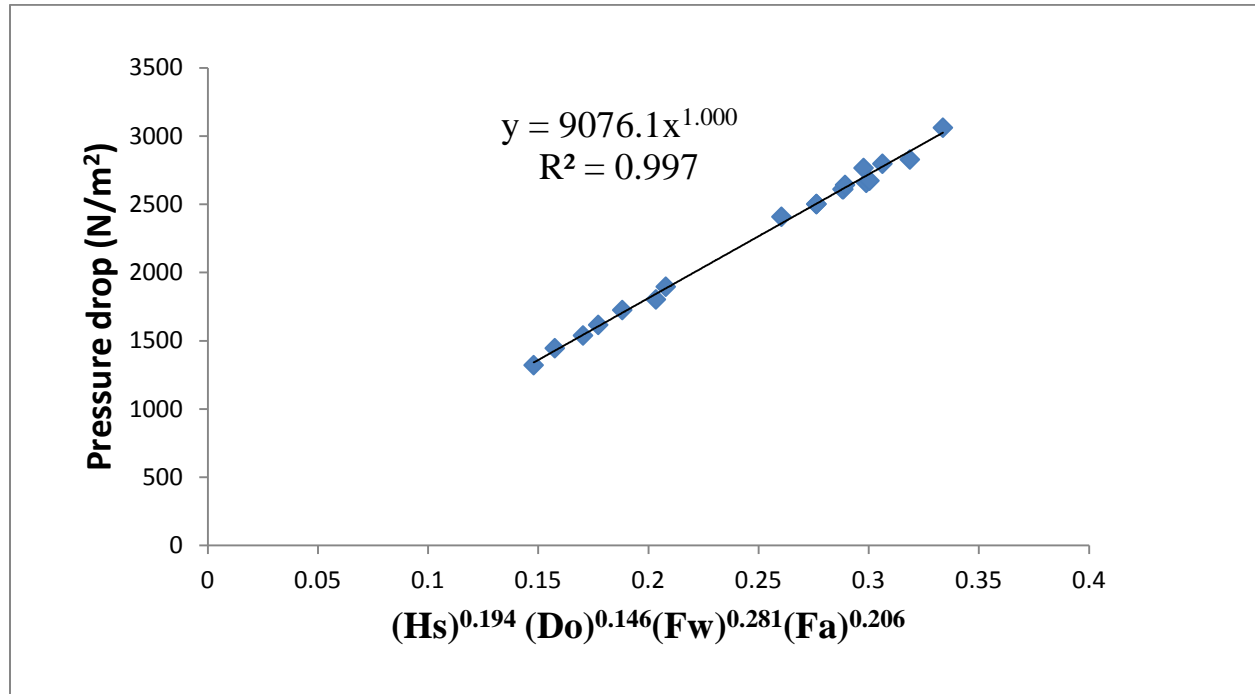


Fig.11. Correlation plot of pressure drop against system parameter

The calculated values of pressure drop by both the methods are found to be agreeing with the experimentally observed values as have been observed from the standard deviations. Observed data and comparison of calculated values with experimental values for both dimensional analysis and statistical analysis are shown in Table-4.4. Standard deviation and mean deviation for this has been listed in Table- 4.6.

Similar procedure was repeated with the pond water considering as the continuous phase for the hydrodynamic studies of Inverse Fluidized. Pressure drop profile against air flow rate (at constant liquid flow rate of 20 lpm) and against water flow rate (at constant air flow rate of 300 lph) are shown in Fig-12 and Fig.-13 respectively. Pressure drop against the bed height measured through different manometers at different liquid flow rates are shown in Fig.-14.

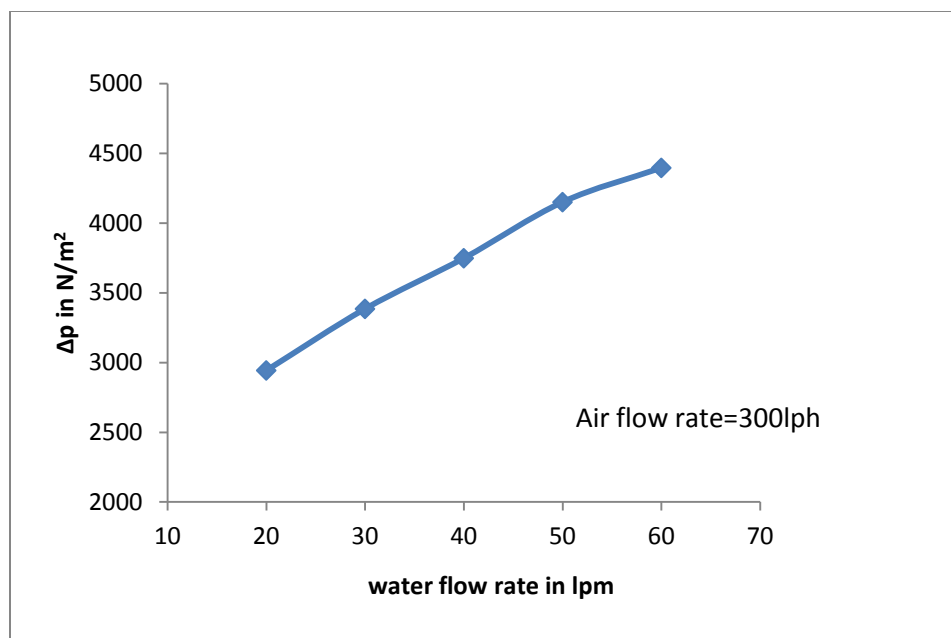


Fig.12. Overall column pressure drop against water flow rate

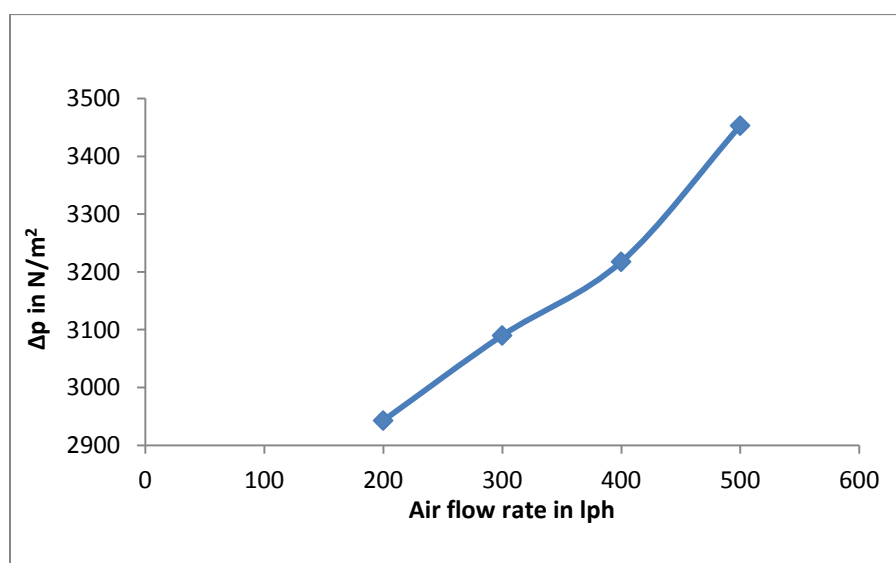


Fig.13. Overall column pressure drop against air flow rate



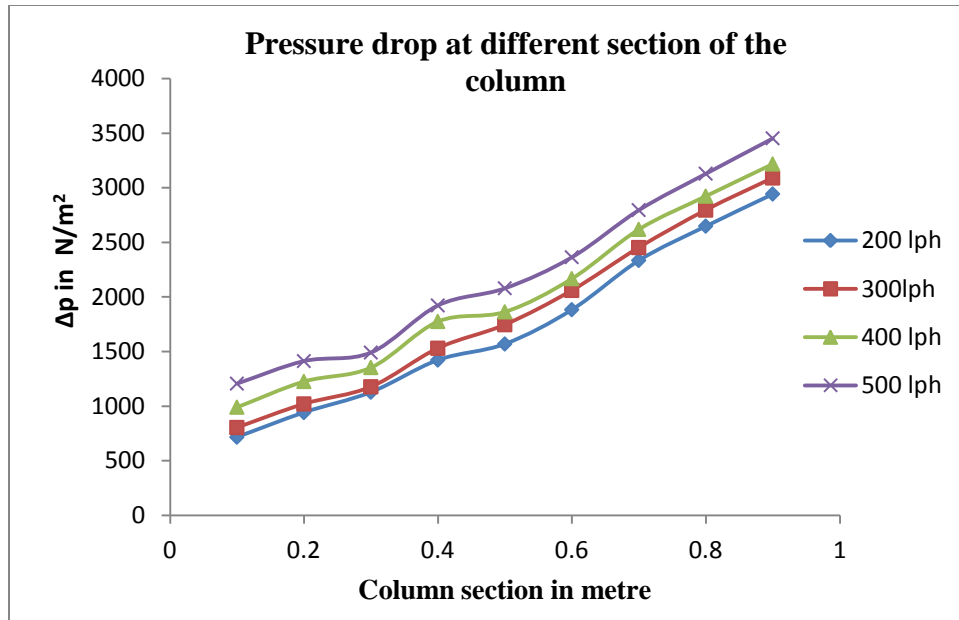


Fig.14. Pressure drop at different levels in the column.

The holdups varied axially for liquid, solid and gas phases are shown in the Figs. 15–18. Solid phase holdups and gas holdups are calculated using Eq-12 and eqn.-10 respectively. Knowing the solid and gas phase hold ups, liquid phase hold up was calculated using Eq-13. The values of all the hold ups are listed in Table-4.1.

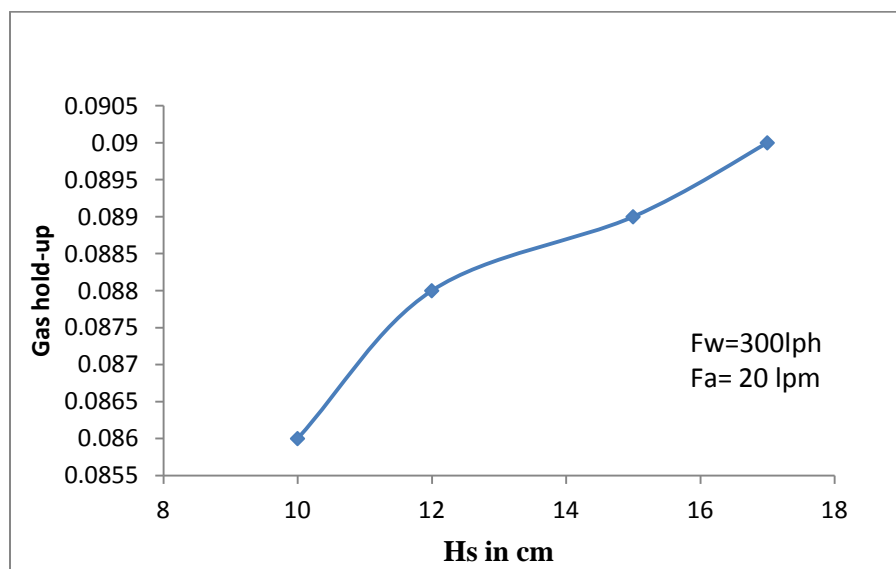


Fig.15. Gas holdup profile against static bed heights

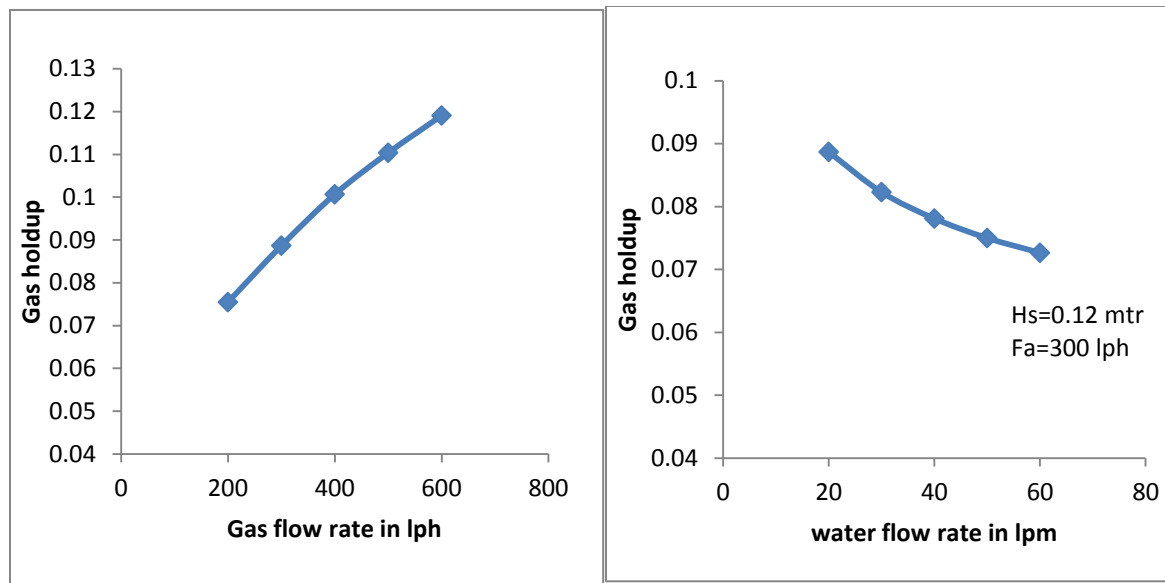


Fig.16. Gas holdup vs. gas flow rate

Fig.17. Gas holdup vs. water flow rate

It is observed fig.18 that gas holdup is higher for higher bed height in constant water and air flow rate. It can also be observed that the gas holdup is relatively small varying between 6% and 12% under the experimental conditions in the present work. It is experimentally observed that more solids are distributed at the top and less at the bottom of the bed.

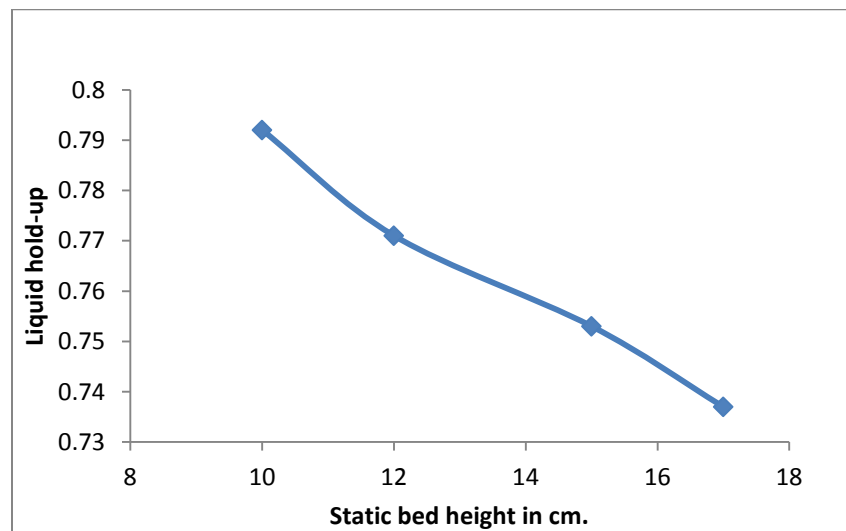


Fig.18. Liquid holdup vs. static bed heights

At constant gas and water flow rate, the liquid holdup is observed to decrease with increasing static bed heights due to the compactness of the bed for more materials under similar conditions (Fig.-18). The variation of solid holdup against different bed heights at a constant gas and liquid flow rate is shown in Fig. 19 .

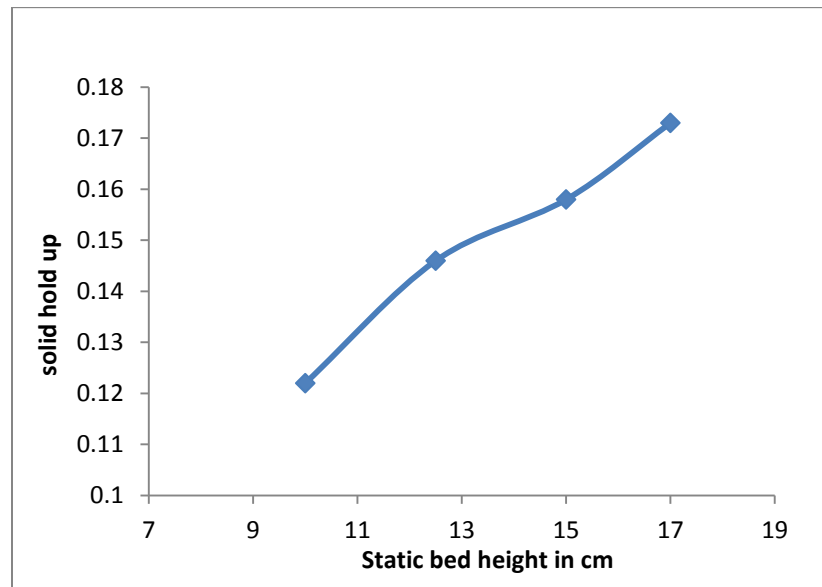


Fig.19. Bed height vs. solid holdup

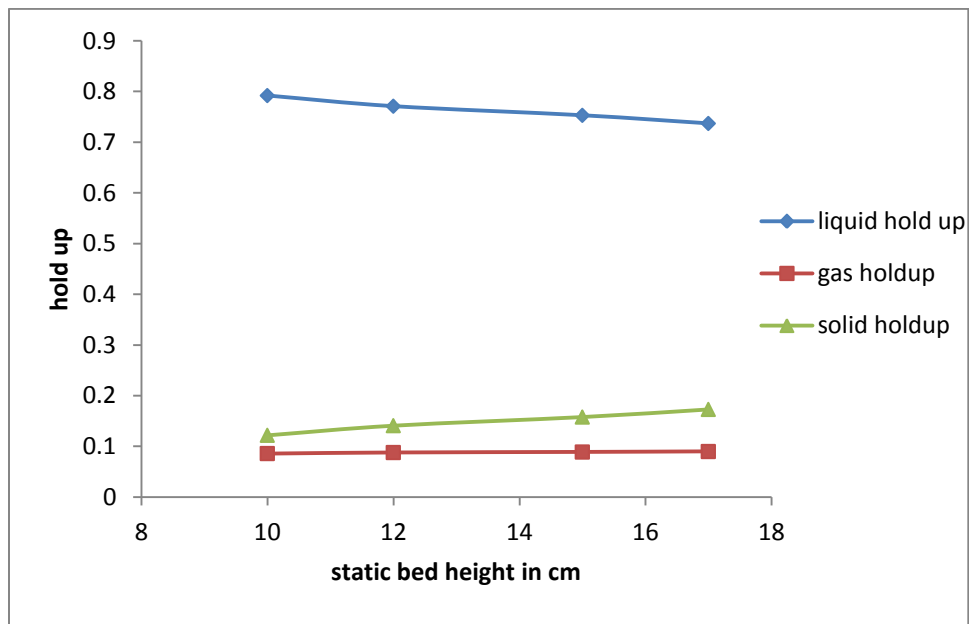


Fig. 20. Holdup profiles against static bed height

Comparison of all three phase holdups against different static bed heights are shown in Fig.-20. It is observed that with increasing bed height the liquid holdup decreases but solid and gas holdups increase with increase in static bed height.

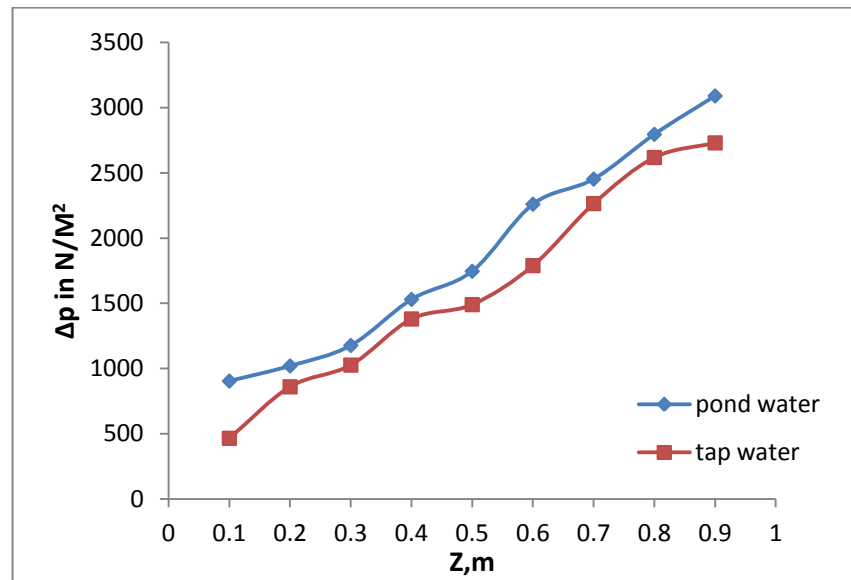


Fig.21. Comparison of pressure drop between pond and tap water

The pressure drop profile measured at different sections of the fluidised bed are compared for pond water and tapwater (with constant liquid flow rate of 20 lpm and air flow rate of 300lph) in Fig.21. It is observed that the pressure drop profile for both the samples (tap water and pond water) follows almost similar trend. The higher pressure drop in case of pond water is due to its slightly higher density (1036 gm/litr) than the normal tapwater.

## 4.2 Biological Treatment Of Industrial Wastewater

Pond water and samples were treated biologically to reduce the pollutants and COD reductions of wastewater were analysed.

### 4.2.1 Results

Attempt has been made to develop a mathematical expression by correlating different system parameters with the experimentally observed COD data for the efficiency of IFB with

respect to COD removal on the basis of dimensional analysis. The developed correlation is as follows.

$$\% \text{ COD removal} = 0.048 [Hs^{0.546} Fw^{0.045} Fa^{0.809}] \quad (17)$$

The developed correlation for % COD removal for steel plant effluent by using statistical analysis is as follows.

$$\% \text{ COD removal} = 59.07 - 4Hs - 2.153Fw + 0.923Hs.Fw - 19.23Fa - 0.153Hs.F - 3.15Fa.Fw + 6.48 Hs.Fw.Fa \quad (18)$$

The calculated values of COD removal for steel plant effluent obtained through these above correlations (developed by both the methods) were compared with the experimental values and comparison was found to be satisfactory (Table-4.5). Standard deviation and mean deviation for this has been listed in Table- 4.6.

## 4.2.2 Discussion:

### 4.2.2.1. Sample-1 : Pond water

Pond water was treated with a mixed culture of microorganisms. The growth kinetics were studied as per the procedure available from literature using spectrophotometer. Optical density of micro-organism culture measured by spectrophotometer is shown in Fig.-22. It is observed that the steady state of growth of microbial culture occurs at around 45 hrs.

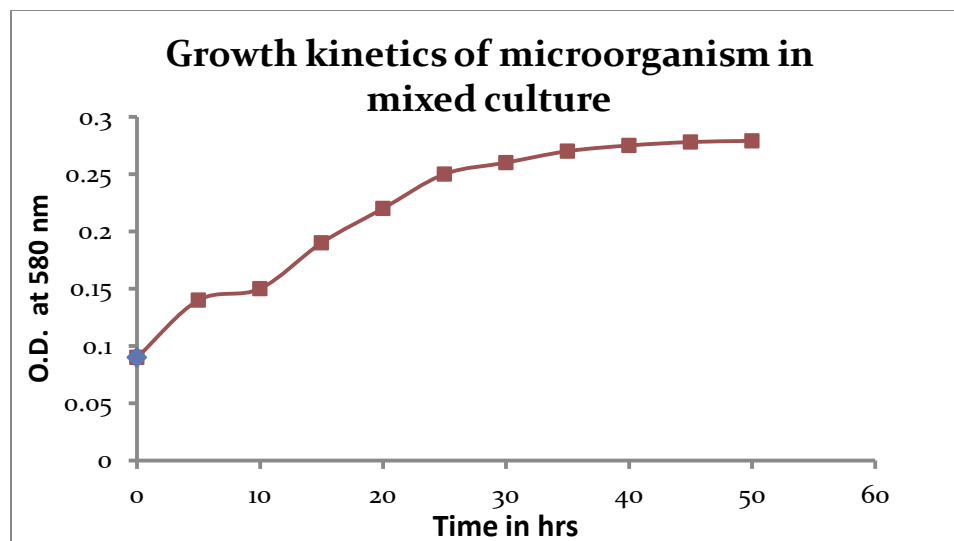


Fig. 22. Optical density measured by spectrophotometer at regular intervals at 580nm of visible light.

The total organic carbon (TOC) content of pond water is determined by toc-analyser. The initial and final TOC ( Total Organic Carbon) were measured and listed in Table-4.2.

### Sample-2 : Effluents from rourkela steel plant

The chemical analysis of the wastewater reveals the following properties of the sample.

Parameters	value
ph	8.6
BOD, 3day at 27 <sup>0</sup> c	34(mg/l)
COD	380(mg/l)
TSS	130(mg/l)

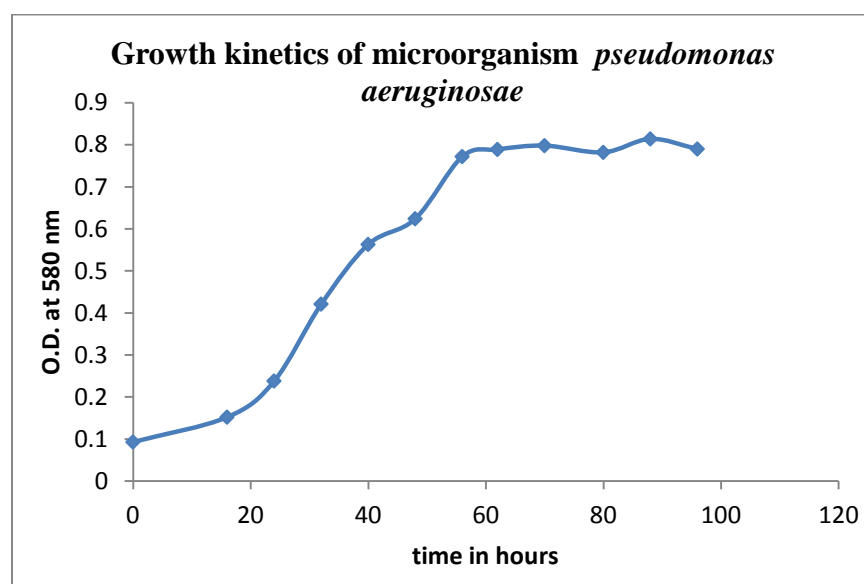


Fig. 23. Growth kinetics of *pseudomonas aeruginosa* culture

Similarly optical density of the second sample (steel plant waste water added with microbial culture) was measured and shown in Fig.-23. From this figure, it can be inferred that the steady state of growth occurs at approximately at 62 hour.

Using cultured sample the fluidised bed was made to run in batch mode initially. The experimentally found COD is plotted against time in regular intervals at  $V_b/V_r = 0.50$  which is shown in fig.-24. As it is found from Fig.-24 that reduction in COD decreased with an increase in  $u$ , attaining the largest value at  $u = 0.034 \text{ ms}^{-1}$ . This can be explained by the fact that with an

increase in oxygen velocity( $u$ ) up to  $0.034\text{ms}^{-1}$ , the aeration conditions for oxygen transfer improved and consequently the amount of the oxygen supplied for biomass growth increased. Bubble size varies little with air velocity and hence an interfacial (air–liquid) area is mainly determined by the air velocity, thus with an increase in  $u$  the interfacial area increased, which was desirable for air–liquid oxygen transfer. For values of  $u$  smaller than  $0.034\text{ms}^{-1}$ , oxygen was the limiting factor for biomass growth. It is noticed in Fig.-24 that an increase in  $u$  above  $0.034\text{ms}^{-1}$  had no effect on reduction in COD values. Thus, for the air velocity of  $0.034\text{ms}^{-1}$ , the degradation rate of the constituents of the wastewaters was the controlling factor for the treatment process.

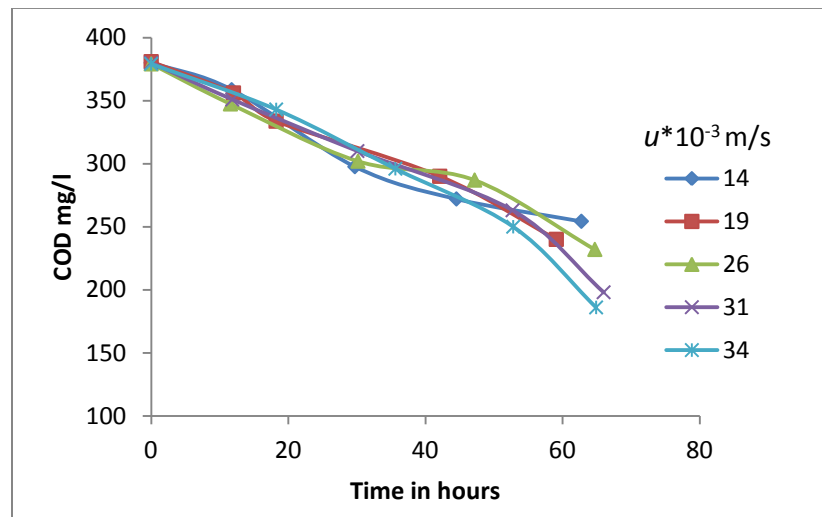


Fig.24. Dependence of COD values on time ( $t$ ) for ratio ( $V_b/V_r$ ) = 0.50 and various oxygen velocities ( $u$ ).

It is also found in Figs 24–26 that for set time  $t$  and ratio ( $V_b/V_r$ ), decrease in COD values depended on the air velocity  $u$ .

It is seen in figures that for a set time  $t$ , decrease in COD values depended on the ratio ( $V_b/V_r$ ) and air velocity  $u$ . It is found in Figs 24-26 that the largest reduction in COD was attained at ( $V_b/V_r$ ) = 0.55. An increase in COD removal with an increase in the ( $V_b/V_r$ ) from 0.50 to 0.55 can be attributed to the fact that for increasing ( $V_b/V_r$ ), more biomass grown on the particles participated in degradation of the constituents of the wastewater. On the other hand, when ( $V_b/V_r$ ) is increased from 0.55 to 0.60, a decrease in COD removal observed with was due to the fact that, in this case, a significant volume of the bioreactor was occupied by the support media and consequently the aeration characteristics of the bed has worsened.

Similarly the COD value is measured at  $V_b/V_r=0.55$  at various oxygen flow rate which are plotted in fig.-25.

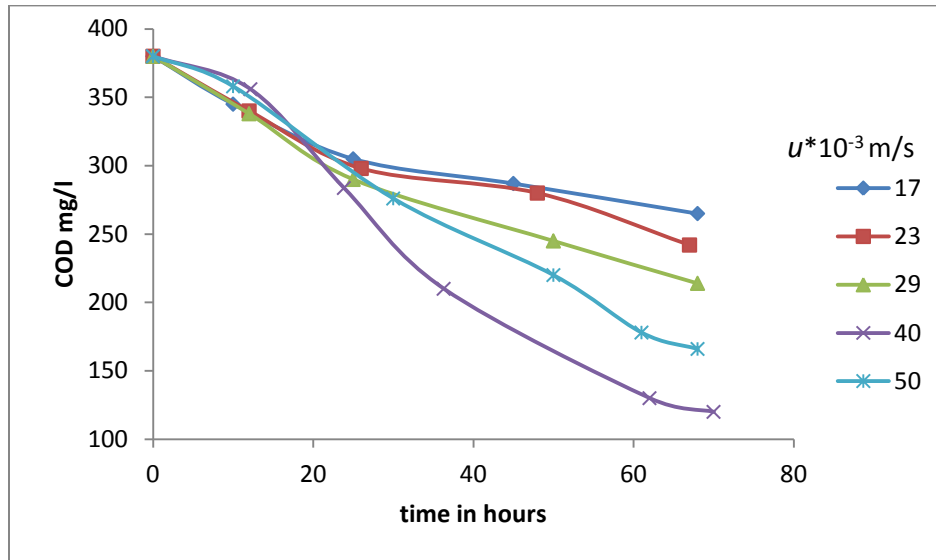


Figure. 25. Relationship between COD values and time ( $t$ ) for ratio ( $V_b/V_r$ ) = 0.55 and various oxygen velocities ( $u$ ).

As it is observed in Figs 24-26, for a set  $t$  the value of  $u$  for which the largest decrease in COD was obtained depended on the ratio ( $V_b/V_r$ ) and hence on volume  $V_b$  of the particles applied in the bioreactor. With the  $V_b$  increasing, the value of  $u$  increased. The large volume of the support can lead to an increase in the amount of the oxygen required for biomass growth and consequently to an increase in the resulting energy cost.

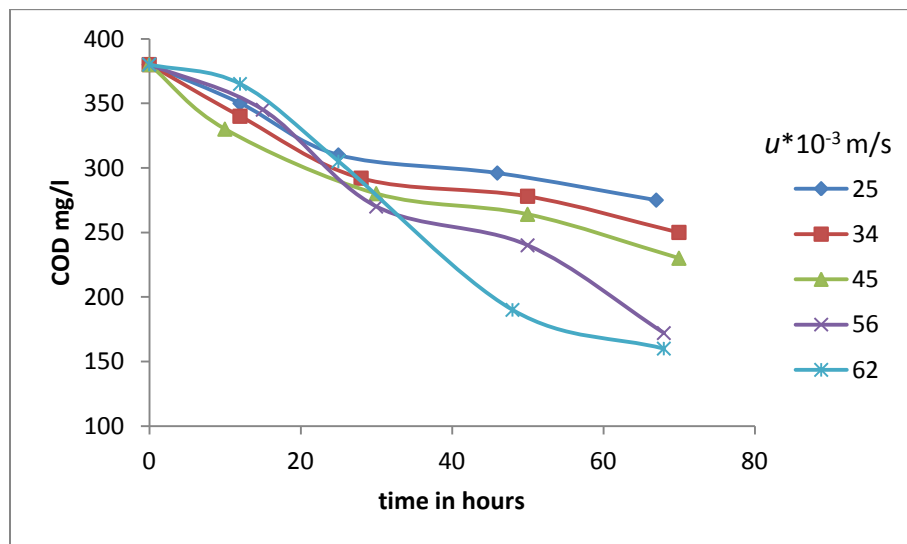
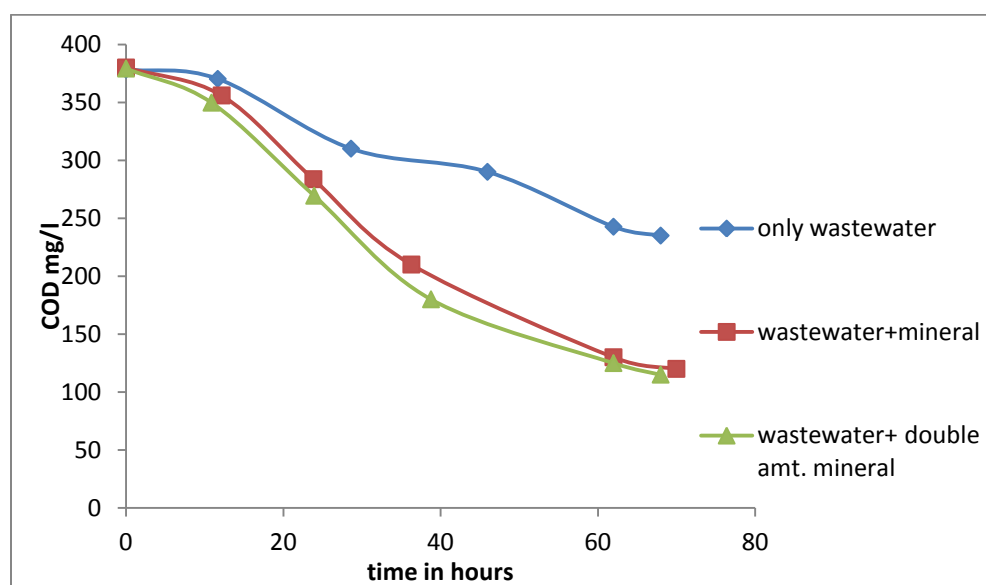


Figure.26. Dependence of COD values on time ( $t$ ) for ratio ( $V_b/V_r$ )= 0.60 and various oxygen velocities ( $u$ ).



Also the COD values for  $V_b/V_r = 0.60$  at various oxygen flow rate are plotted in Fig.-60. It is noted that for a particular residence time  $t$ , the smallest value of COD and hence the largest COD reduction was achieved when the bioreactor was maintained at  $(V_b/V_r) = 0.55$  and  $u = 0.040 \text{ ms}^{-1}$ .

The comparison plot for COD removal for only wastewater, wastewater enriched with minerals and wastewater enriched with double amount of minerals is given in Fig.-27. Also it is observed in Fig. 27 that in treatment of 'raw' wastewater value of COD decreased from 380 to 235 mg/l, which is, only about 40% COD removal. In the operation where wastewater added with nutrient salts was used, a decrease in COD from 380 to 120 mg/litre was obtained, that is, approximately 68% COD reduction. It is also noted in Fig.-27 that no improvement in treatment efficiency was achieved in the operation with wastewaters enriched in the double amount of nutrient salts. Thus, the recommended amount of mineral salts was sufficient for biomass growth when added to wastewater before treatment.



**Figure 27.** Comparison of cod removal at optimum condition

It is observed that the phenolic constituents of the wastewater were successfully degraded in the bioreactor. The use of low density particles in a bioreactor allowed the control of biomass loading in the apparatus.

Further the inverse fluidised bed was operated in continuous mode where the wastewater sample is recirculated in a complete loop. The COD measured at regular intervals at optimum conditions in continuous mode is plotted in fig.-28.

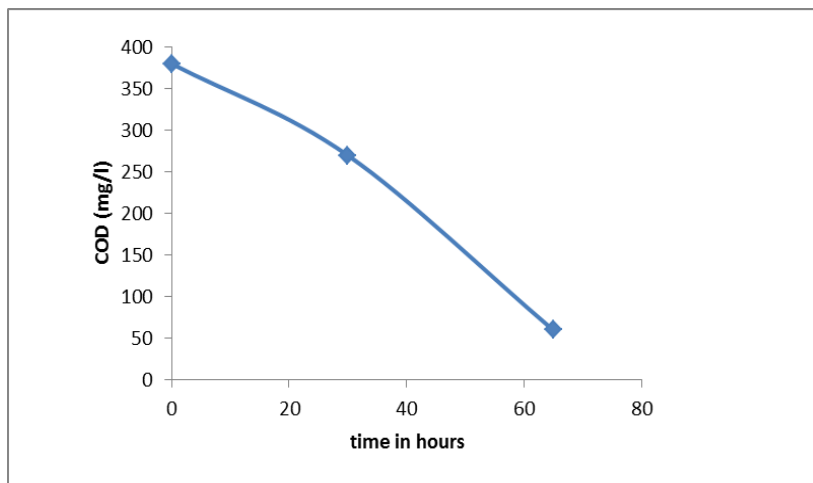


**Fig.28.** COD removal efficiency for continuous mode at optimum conditions.

In continuous culture mode the COD removal efficiency was found out to be 84.2 % which is greater in comparison to batch mode.

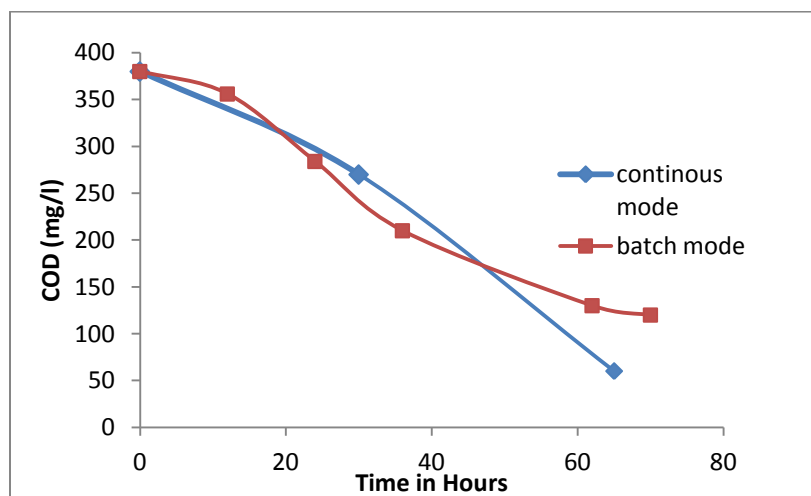


**Fig.29.** Comparison of COD removal efficiency of batch culture mode with continuous mode.

Also a comparison is made between COD removal efficiency of batch culture mode with continuous mode (Fig.-29). In case of continuous mode the COD removal efficiency is larger than the batch mode.

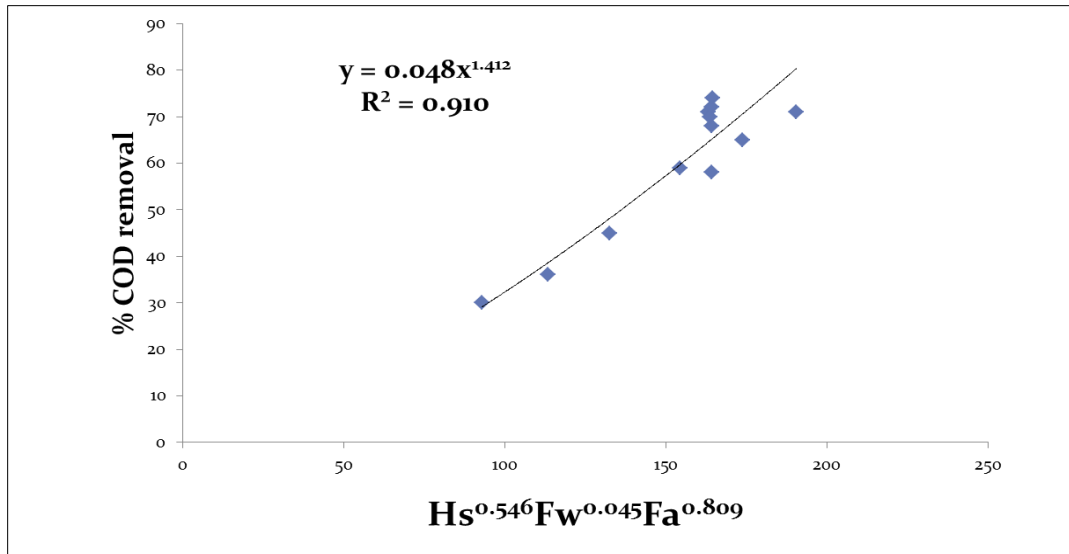


**Fig.30.** Correlation plot of percentage COD removal against system parameter

Correlation plot for the % COD removal against the system parameters is shown in Fig.-30.

The calculated values of % COD removal by both the dimensional analysis and statistical analysis methods are found to be agreeing with the experimentally observed values as have been observed from the standard deviations. The standard deviation and mean deviation for both the method is depicted in Table-6. Observed data and comparison of calculated values with experimental values for both dimensional analysis and statistical analysis are shown in Table-7.

The properties of the sample effluents of steel plant after biological treatment in inverse fluidised bed bioreactor were mentioned in Table-4.3.

**Table 4.1 :** Three phase holdups measured at different static bed heights.

$H_s$ ( in cm.)	$\varepsilon_s$	$\varepsilon_l$	$\varepsilon_g$
10	0.122	0.792	0.086
12	0.141	0.771	0.088
15	0.158	0.753	0.089
17	0.173	0.737	0.09

**Table 4.2.** Initial and final TOC of pondwater

	Initial TOC (ppm)	Final TOC(After 48hr) (ppm)	TOC removal efficiency(%)
without adding nutrients	1982.3	1307.1	34.06
After adding nutrients	2156	838.2	61.12

**Table 4.3:** Properties of sample-2 (steelplant effluents) after treatment.

Parameters	Initial value	Final value
ph	8.6	7.3
BOD, 3day at 27 <sup>0</sup> c	34(mg/l)	14(mg/l)
COD	380(mg/l)	60(mg/l)
TSS	130(mg/l)	94(mg/l)

**Table.4.4:** Observed data & comparison of calculated values of pressure drop with experimental values.

Sl.No.	Static bed height Hs(cm)	Distributor size Do(mm)	Water flow Rate $F_w \times 10^{-3}$ (m <sup>3</sup> /sec)	Air flow rate $F_a \times 10^{-3}$ (m <sup>3</sup> /sec)	$\Delta P_{exp}$ (N/m <sup>2</sup> )	Dimensional analysis		Statistical analysis	
						$\Delta P_{cal}$	% dev	$\Delta P_{cal}$	% dev
1	12.5	3	1.84	555.556	2610.559	2615.817	-0.20	2923.95	-12.2
2	15	3	1.84	555.556	2657.176	2710.081	-1.99	2884.89	-8.58
3	17	3	1.84	555.556	2797.027	2776.752	0.72	2802.964	-11.96
4	10	2	1.84	555.556	2408.551	2360.79	1.98	2167.5	-10.08
5	10	4	1.84	555.556	2610.559	2612.446	-0.07	2212.18	15.24
6	10	5	1.84	555.556	2765.949	2699.037	2.41	2516.5	9.41
7	10	3	2.00	555.556	1320.818	1340.713	-1.50	1135.6	-14.98
8	10	3	2.50	555.556	1445.131	1427.68	1.20	1618.5	-12.04
9	10	3	3.30	555.556	1538.365	1543.8	-0.35	1307.606	15.07
10	10	3	3.80	555.556	1616.06	1606.378	0.59	1400.7	-3.45
11	10	3	4.70	555.556	1724.833	1705.487	1.12	1499.88	-13.70
12	10	3	6.20	555.556	1802.529	1843.866	-2.29	1567.64	13.84
13	10	3	6.70	555.556	1895.763	1884.588	0.58	1667.6	-12.05
14	10	3	1.84	555.55	2501.7	2504.8	-0.12	2289.05	8.54
15	10	3	1.84	555.556	2501.785	2504.8	-0.12	2411.7	3.98
16	10	3	1.84	694.444	2641.637	2622.8	0.71	2609.88	1.29
17	10	3	1.84	833.333	2672.715	2723.3	-1.89	2912.48	-9.62
18	10	3	1.84	111.111	2828.105	2889.7	-2.17	2748.91	2.8
19	10	3	1.84	138.888	3061.191	3025.793	1.15	3428.432	-12.23

**Table.4.5:** Observed data & comparison of calculated values of COD removal efficiency with experimental values.

Sl. no.	Static bed height Hs(cm)	water flow rate Fw(lph)	oxygen flow rate Fa(m <sup>3</sup> /sec)	% COD removal exp	Dimensional analysis		Statistical analysis	
					% COD removal calculated	% dev	% COD removal calculated	% dev
1	50	40	80	59	58.598	-0.20	79.999	-21.21
2	55	40	80	68	63.637	-1.96	84.919	-24.88
3	60	40	80	65	68.614	0.72	84.307	-29.70
4	55	17	80	30	29.695	1.98	63.999	-6.66
5	55	23	80	36	38.871	-0.072	52.305	6.59
6	55	29	80	45	47.786	2.41	27.693	7.69
7	55	40	80	58	63.637	-1.50	35.693	10.76
8	55	40	80	71	77.631	1.20	43.693	12.61
9	55	40	40	71	63.05	-0.35	79.999	-12.67
10	55	40	60	70	63.393	0.59	84.919	-21.31
11	55	40	80	72	63.637	1.12	84.307	-17.09
12	55	40	100	74	63.827	-2.29	63.999	13.51
13	45	40	80	49	53.492	0.58	52.305	-6.74

**Table.4.6** Standard deviation and Mean deviation of calculated values with experimental values.

	Dimensional Analysis		Statistical Analysis	
	Standard deviation	Mean deviation	Standard deviation	Mean deviation
Pressure drop	1.406	-0.01	10.1	-2.6
% COD Removal	8.923	0.17	15.93	-6.8

## **CHAPTER-5**

## **CONCLUSION**

From experimentation with the gas–liquid–solid inverse fluidized bed bioreactor containing polypropylene particles, the following conclusions can be drawn:

- Different hydrodynamics properties mainly the bed pressure drop and hold ups of inverse fluidized bed are studied for both tap water and pond water. Higher pressure drop for pond water indicates that treatment of waste water needs more power as pressure drop is more. Accordingly the steps were taken for the selection of the micro organism for development of bio film on the bed material.
- The ph of the steel industry effluent after microbial treatment is reduced to 7.3 from 8.6 which is nearer to neutral range ph of water.
- Reduction in COD depended on ratio ( $V_b/VR$ ), air velocity  $u$  and residence time  $t$ . For set  $t$  and  $u$ , reduction in COD initially increased, and then decreased with an increase in ( $V_b/VR$ ), attaining the largest value at  $(V_b/VR) = 0.55$ . Similarly, for set  $t$  and ( $V_b/VR$ ), reduction in COD initially increased monotonically, and then decreased with an increase in gas flow. These changes have been attributed to interplay of surface area and oxygen limitations.
- Optimal operation, on the basis of largest COD removal, was achieved when the bioreactor was controlled at the ratio  $(V_b/VR) = 0.55$  and an air velocity  $u = 0.040 \text{ ms}^{-1}$ . Under these conditions, COD was practically constant after 62 h. At this steady state, batch culture mode only about 40% COD removal was obtained in the treatment of wastewater without adding any minerals, whereas in the operation with the addition of mineral salts to wastewaters, approximately 68% COD removal efficiency was obtained. The following amount of nutrient salts (mg/litre):  $(\text{NH}_4)_2\text{SO}_4$ —500;  $\text{KH}_2\text{PO}_4$ —200;  $\text{MgCl}_2$ —30;  $\text{NaCl}$ —30;  $\text{CaCl}_2$ —20; and  $\text{FeCl}_3$ —7, when added to wastewater before treatment, was sufficient for biomass growth.
- When the reactor was operated in continuous culture mode almost 84% COD reduction was achieved. Therefore inverse fluidised bed can be used as an effective bioreactor to treat industrial effluents biologically.



**NOMENCLATURE**

$H_s$	:Initial static bed height, m
$\varepsilon_g$	:Gas holdup in fluidized bed
$\varepsilon_l$	:Liquid holdup in fluidized bed
$\varepsilon_s$	:Solid holdup in fluidized bed
$U_g$	:Superficial gas velocity, $\text{m s}^{-1}$
$U_L$	:Superficial liquid velocity, $\text{m s}^{-1}$
$U_{mf}$	:Minimum fluidization velocity, m/s
Re	:Bubble Reynolds number
$Hr$	:Bed aspect ratio ( $= H_s/ D_c$ )
$N$	:Richardson-zaki index
$Ar$	:Archimedes number
$k_{La}$	:Mass transfer coefficient
$\delta$	: biofilm thickness
$\varepsilon$	: holdup (volumetric fraction)
$\mu$	: specific growth rate , viscosity( $\text{kg m}^{-1} \text{s}^{-1}$ )
COD	: chemical oxygen demand
$V_b$	:Bed volume
$V_r$	:Reactor volume

## REFERENCES:

- [1] Arnaiz , C., Buffiere , P., Lebrato , J., and Moletta, R., The effect of transient changes in organic load on the performance of an anaerobic inverse turbulent bed reactor, *Chemical Engineering and Processing* 46 (2007) 1349–1356.
- [2] Benedict and Moletta ; (1999). Some hydrodynamic characteristics of inverse three fluidized bed reactors. *Chemical Engineering Science*, 54, 1233-1242.
- [3] Briens, C. L., Ibrahim, Y.A A., Margaritis, A., and Bergougnou, M. A., Effect of coalescence inhibitors on the performance of three-phase inverse fluidized-bed columns, *Chemical Engineering Science* 54 (1999) 4975-4980.
- [4] Chen, X. and Zheng, P.;(2009).Bed expansion behavior and sensitivity analysis for super-high-rate anaerobic bioreactor; *univ-sci b (biomed & biotechnol)* 2010 11(2):79-86.
- [5] Chern, H. S., Muroyama, K. and Fan, L.S.:(1982). Hydrodynamics of constrained inverse fluidization and semi-fluidization in a gas-liquid-solid system, *Chemical Engineering Science*, 38(8), 1167-1174.
- [6]Comte, M. P., Bastoul, D., Hebrard, G., Roustan, M. and Lazarova, V., Hydrodynamics of a three-phase fluidized bed the inverse turbulent bed, *chemical engineering science*,. Vol. 52.Nos, 21 22, pp. 3971-3977, 1997.
- [7] Das, B., Ganguly, U., Das,S., Inverse fluidization using non-Newtonian liquids, *Chemical Engineering and Processing* (2010).
- [8] Fan, L., Katsuhiko, M. and Chern, S., Hydrodynamic Characteristics of Inverse Fluidization in Liquid-Solid and Gas-Liquid-Solid Systems, *The Chemical Engineering Journal*, 24 (1982) 143 – 150.
- [9] Fan, L., Katsuhiko, M. and Chern, S., Some remarks on hydrodynamics of inverse gas-liquid-solid fluidization, *Chemical Engineering science* Vol. 31. No. 10.pp. 1570-1572, 1982.
- [10] Fuentes, M., Scenna N. J., Aguirre , A. and . Mussati M. C., ;(2007) Hydrodynamic aspects in anaerobic fluidized bed reactor modeling; *Chemical Engineering and Processing* 47, 1530–1540
- [11] Garcia, D., Buffiere, P. Molettal, R., and Elmaleh, S., Anaerobic digestion of wine distillery wastewater in down-flow fluidized bed, *Wat. Res.* Vol. 32, No. 12, pp. 3593-3600, 1998.

- [12] Gomez, L., Bodalo, A., and Gomez, E.,(2006) Murcia Experimental behaviour and design model of a fluidized bed reactor with immobilized peroxidase for phenol removal *Chemical Engineering Journal* 127 ,47–57
- [13] Han, S. J., Tan, R. B. H., and Loh, K. C., Hydrodynamic behaviour in a new gas-liquid-solid inverse fluidization airlift bioreactor, *Trans IChemE*, Vol 78, Part C, December 2000.
- [14] Karamanev, D. G. and Nikolov, L. N., 1992, Bed expansion of liquid-solid inverse • fluidization, *AIChE J*, 38: 1916.
- [15] Karamanev, D.G. , Nagunume, T., and Endo, K., Hydrodynamics and mass transfer study of a gas–liquid–solid draft tube spouted bed bioreactor. *ChemEngSci***47**:3444–3450 (1992).
- [16] Krishna S.V., S.R. Bandaru, D.V.S. Murthy, K. Krishnaiah;(2003), some hydrodynamic aspects of 3-phase inverse fluidized bed, *ChinaParticology*, 5, 351–356
- [17] Krishnaiah, K., Guru, S. and Sekar,V., Hydrodynamic studies on inverse gas-liquid-solid fluidization, *The Chemical Engineering Journal*, 51 (1993) 109-112.
- [18] Krishna, S.V. , Bandaru, S. R., and Murthy, D.V.S., Some hydrodynamic aspects of 3-phase inverse fluidized bed, *China Particuology* 5 (2007) 351–356.
- [19] Mukherjee, A.K., Mishra, B.K., and Kumar R.V., Application of liquid/solid fluidization technique in beneficiation of fines, *Int. J. Miner.Process.* 92 (2009) 67–73.
- [20] Nikolov V., Farag L., and NikovI.; (2000), Gas-liquid mass transfer in a bio-reactor with three phase inverse fluidized bed . *Bioprocess Engineering*, 23, 427- 429.
- [21] Nore, O., Briens, C., Margaritis, A. and Wild, G.,Hydrodynamics of gas–liquid mass transfer and particle–liquid heat and mass transfer in a three-phase fluidized bed for biochemical processapplications. *ChemEngSci***47**:3573–3580 (1992).
- [22] Reese, J., Ellen, M., Shang, Y., and Fan, L., Industrial Applications of Three-Phase Fluidization Systems. Fluidization, Solid Handling, and Processing, Industrial Applications 1998, Pages 582-682.
- [23] Renganathan T. and Krishnaiah, K.; (2005), Voidage characteristics and prediction of bed expansion in liquid–solid inverse fluidized bed, *ChemEnggSc*, 60, 2545 – 2555
- [24] Renganathan, T. and Krishnaiah, K., Liquid phase mixing in 2-phase liquid–solid inverse fluidized bed, *Chemical Engineering Journal* 98 (2004) 213–218.

- [25] Sanchez ,O., Michaud, S., Escudi, R., and Bernet, N., Liquid mixing and gas–liquid mass transfer in a three-phase inverse turbulent bed reactor, *Chemical Engineering Journal* 114 (2005) 1–7.
- [26] Shieh, W. and Keenan, D., Fluidized bed biofilm reactor for wastewater treatment, in *Advances in Biochemical Engineering/Biotechnology*, vol 33 ed by Fiechter A. Springer, Berlin Heidelberg, pp, 132–168 (1986).
- [27] Show K., Lee, U., Chang ,J.S. ;(2011). Bioreactor and process design for biohydrogen production; *Bioresource Technology*,.
- [28] Sokol, Korpál, Aerobic treatment of wastewaters in the inverse fluidized bed reactor. *Chemical Engineering journal*, 118, 199-205.
- [29] Sokół, W., Operating parameters for a gas–liquid–solid fluidized bed bioreactor with a low density biomass support. *BiochemEng J* 8:203–212 (2001).
- [30] Sokol, W. and Korpál, W., Aerobic treatment of wastewaters in the inverse fluidized bed biofilm reactor, *Chemical Engineering Journal* 118 (2006) 199–205.
- [31] Sowmeyan , R., Swaminathan, G.:(2007)Evaluation of inverse anaerobic fluidized bed reactor for treating high strength organic wastewater; *Bioresource Technology* 99 ,3877–3880.
- [32] Sowmeyan, R. , and Swaminathan, G., Evaluation of inverse anaerobic fluidized bed reactor for treating high strength organic wastewater, *Bioresource Technology* 99 (2008) 3877–3880.
- [33] Sung, M.S., Suk H. K. , Kim,U., Yong, K., and Sang,D., Bubble properties in three-phase inverse fluidized beds with viscous liquid medium, *Chemical Engineering and Processing* 46 (2007) 736–741.
- [34] Vijayalakshmi, Balamurugam, Sivakumar, Samuel, Velan;(2000). Minimum fluidization velocity and friction factor in a liquid-solid inverse fluidized bed reactor.*Bioprocess Engineering*, 22, 461-466.
- [35] Verstraete W.and Vaerenbergh, E., Aerobic activated sludge, in *Biotechnology*, vol 8, ed by Schonborn W (series edsRehm H-J and Reed G). VCH VerlagsgesellschaftmbH, Weinheim, pp 43–112 (1986).
- [36] Wang, D., Silbaugh, T., and Pfeffer,R., Lin, Y.S., Removal of emulsified oil from water by inverse fluidization of hydrophobic aerogels, *Powder Technology* 203 (2010) 298–309.
- [37]W. Volk, (Second Edition), ‘Applied Statistics for Engineers’ McGraw-Hill,Inc,USA, 1969, p-237 and 336.

- [38] Yang, G.Q., Du, B., and Fan, L.S., Bubble formation and dynamics in gas–liquid–solid fluidization—A review, *Chemical Engineering Science* 62 (2007) 2 – 27.